Title: From nano to micrometer size particles - A characterization of airborne cement particles during construction activities.

Authors: Batsungnoen K, Riediker M, Suárez G, Hopf NB

Journal: Journal of hazardous materials

Year: 2020 May 23

Issue: 398

Pages: 122838

DOI: 10.1016/j.jhazmat.2020.122838

From nano to micrometer size particles – a characterization of airborne cement particles during construction activities

Kiattisak Batsungnoen[1,2], Michael Riediker[3], Guillaume Suárez[1], Nancy B Hopf[1]

1. Center for Primary Care and Public Health (Unisanté), University of Lausanne, Switzerland. (kiattisak.batsungnoen@unisante.ch, nancy.hopf@unisante.ch, guillaume.suarez@unisante.ch)
2. Institute of Public Health, Suranaree University of Technology, Thailand
3. Swiss Centre for Occupational and Environmental Health (SCOEH), Winterthur, Switzerland. (michael.riediker@alumni.ethz.ch)

Corresponding author: Nancy B Hopf, PhD

Keywords: Photocatalytic cement, Nano cement, Nano TiO_2, Photocatalytic cement exposure, Nano TiO_2 exposure, Cement particle exposure

Abstract

Although, photocatalytic cement contains nanosized TiO_2, a possibly carcinogen, no exposure assessments exist for construction workers. We characterized airborne nanoparticle exposures during construction activities simulated in an exposure chamber. We collected some construction site samples for regular cement in Switzerland and Thailand for comparison. Airborne nanoparticles were characterized using scanning mobility particle sizer (SMPS), portable aerosol spectrometer (PAS), diffusion size classifier (DiSCmini), transmission electron microscopy (TEM), scanning electron microscope energy dispersive X-ray spectroscopy (SEM-EDX), and X-ray diffraction. Bagged photocatalytic cement had 2.0 wt% (GSD±0.55) TiO_2, while TiO_2 in aerosols reached 16.5 wt% (GSD±1.72) during bag emptying and 9.7 wt% (GSD±1.36) after sweeping. The airborne photocatalytic cement particles were far smaller (approximately 50 nm) compared to regular cement. Cutting blocks made from photocatalytic cement or concrete, resulted in similar amounts of airborne nano TiO_2 (2.0 wt% GSD±0.57) particles as in bagged material. Both photocatalytic and regular cement had a geometric mean diameter (GMD) < 3.5 µm. Main exposures for Thai workers were during sweeping and Swiss workers during drilling and polishing cement blocks. Targeted nanoparticle exposure assessments are needed as a significantly greater exposure to nano TiO_2 were observed than what would have been predicted from the material's nano- TiO_2 contents.

1. Introduction

An increasing number of nanotechnology-based products are making its way into the construction sector (Zhu et al., 2004). One such product is photocatalytic cement made by adding nano-scaled (less than 100 nm in size) titanium dioxide (TiO_2) particles. This gives the cement self-cleaning properties (Lan, Lu, and Ren 2013; Paz et al. 1995). The increasing use of nanomaterials have led to an increased need for hazard and exposure information on these materials in order to anticipate, recognize, evaluate, and control factors in the workplace, which otherwise may cause impaired health among workers.

TiO_2 was classified as "possibly carcinogenic to humans" (class 2B) by the International Agency for Research on Cancer (IARC) (IARC, 2017; WHO, 2010). In the U.S., the National Institute for Occupational Safety and Health (NIOSH) provided a more nuanced assessment by classifying only ultrafine (nanoscale) TiO_2 as a potential carcinogen, while considering the data to be insufficient for making such a statement for fine (larger) TiO_2 (NIOSH, 2011). The hazard associated with exposures to nano-sized TiO_2 particles (nano TiO_2) has been reported by a series of studies (NIOSH, 2009). Nano TiO_2 was found to increase reactive oxygen species (ROS) production (Arenberg and Arai 2020; H. Ma, Brennan, and Diamond 2012; Sayes et al., 2006; Lee et al., 2010; Long et al., 2006), and induce DNA damage (Falck et al., 2009; Ghosh et al., 2010; WHO, 2010; Sha et al., 2015) and cell toxicity (C. Xue, Luo, and Yang 2015; Sha et al., 2015; Lee et al., 2010 Sayes et al., 2006). Furthermore, nano TiO_2 can be translocated to different organs and accumulate in the kidneys, lymph nodes, heart, liver, and brain (Wang et al., 2008; Kreyling et al., 2010; Geiser and Kreyling, 2010; Shi et al., 2013; Shinohara et al. 2015).

Nano TiO_2 particles are highly photoreactive. They react with organic and inorganic gases (Chen and Poon 2009; Lim et al. 2000; Dalton et al. 2002; Diesen and Jonsson 2014; Fujishima and Zhang 2006) and induce phototoxicity in microorganisms (Lan et al., 2013; Carp et al., 2004; Banerjee et al., 2015; Chen and Poon, 2009; Lee et al., 2010; Zhi Ge and Zhili Gao, 2008). This biocidal effect is one of the reasons why nano TiO_2 is an interesting additive because it renders building surfaces "self-cleaning" because it kills any organic growth.

Photocatalytic cement is mainly regular cement with TiO_2 nanoparticles and additives. Regular cement has been used since the Roman era to build strong structures by mixing cement with water, rock, and sand (Edwin G. Foulke, 2008). Only 2-3 wt% nano TiO_2 were added to cement to produce photocatalytic cement (Ma et al. 2015; Jimenez-Relinque et al., 2015; Batsungnoen et al., 2019). The particle size distributions of aerosolized photocatalytic cement generated during work activities are not known. Given that nano TiO_2 is not chemically bound to the cement particles, they might still behave like nanoparticles, and may easily be released (Aitken et al., 2004; Ostiguy et al., 2006; Friedlander and Pui, 2003; Ding et al., 2017).

The risk for work related diseases over a lifetime in a construction trade is 2–6 times greater compared to non-construction work. About 16% of construction workers develop chronic obstructive pulmonary disease (COPD) (Ringen et al., 2014). Cement dust exposures are one of the health concerns. They are generated during many construction activities (van Deurssen et al., 2014) such as abrasive blasting, bag emptying, cement mixing, concrete drilling, concrete block cutting, sawing, and sweeping. Inhalation is the most common route of entry for airborne cement as well as for nanoparticles. Inhaled cement dust can lead to multiple lung diseases such as chronic respiratory symptoms, lung function impairment, bronchitis, COPD, pneumoconiosis, silicosis, and lung cancer (Eom et al., 2017; Maciejewska and Bielichowska-

Cybula, 1991; Meo, 2004; Penrose, 2014; Nordby et al., 2011; Yang et al., 1996; Moghadam et al., 2017).

Cement also contains silicon dioxide (SiO_2). Crystalline silica, as quartz and cristobalite, are carcinogenic to humans (IARC, 2012; IARC, 2017; IARC, 1997). Moreover, crystalline silica causes chronic bronchitis, COPD, and silicosis (Kaewamatawong et al., 2005; Napierska et al., 2010; Soutar et al., 2000). Higher concentrations of amorphous silica might cause pneumoconiosis, granuloma formation, reversible inflammation, and emphysema (McLaughlin et al., 1997; Merget et al., 2002; Kaewamatawong et al., 2005). For crystalline silica, NIOSH recommends an exposure limit of 0.05 mg/m^3 (OSHA, 2018), and for amorphous silica 6 mg/m^3 (NIOSH, 2018).

The construction industry employs millions of workers. Many die or suffer from occupational diseases arising from accumulated exposure to hazardous substances (ILO, 2014). Managing hazardous exposures properly can reduce the burden of disease, but can only be done effectively if exposures have been characterized. Currently, there are no studies characterizing airborne nano TiO_2 in cement during work activities.

Our aim was to characterize airborne nano- and micrometer particle exposures during typical construction work activities for photocatalytic and regular cement. Our results can be directly used in developing risk management strategies among construction workers using photocatalytic cement. In addition, it will enhance our understanding of airborne nanoparticles and their size distributions, concentrations, and morphologies in mixtures with other particles.

2. Materials and methods

Materials

Portland cement type I (cement-clinker; CE number 266-043-4) was obtained from Jura cement (Wildegg, Switzerland). Photocatalytic cement was acquired as a sample from the manufacturer (TX-Active®, Italcementi group, Nazareth, US). Fine sand used to make concrete was bought from a general home improvement store in Switzerland.

Characterization of the two cement types

Airborne particles were characterized by assessing their size distribution, number and mass concentration, morphology, phase analysis, and elemental composition. The instruments and measurement techniques used are shown in Table 1. Airborne nanoparticle concentrations and size distributions were measured with three different devices: the size distribution in the range from 11 to 1,083 nm was measured with a scanning mobility particle sizer (SMPS; model SMPS+C model 5400, Grimm Aerosol Technik GmbH & Co. KG, Ainring, Germany); the size distributions in the range from 250 to 32,083 nm with a portable aerosol spectrometer (PAS; model 1.109, Grimm Aerosol Technik GmbH & Co. KG, Ainring, Germany); and the fast (1 Hz) particle number count concentration in the range from 10 to 700 nm with a diffusion size classifier (DiSCmini; Testo North America, West Chester, PA USA). Elemental composition was determined by scanning electron microscope energy dispersive X-ray spectroscopy (SEM-EDX) (SEM-EDX; PHENOM XL BSE detector at 15kV). The SEM-EDX analysis returns the atomic and weight concentrations. Composition of objects as small as 10 nm can be assessed with SEM-EDX analysis. We averaged the results of three randomly selected wide scanning surface zones (15x15 µm) to calculate the weight percent for each element (wt%). Bagged material was analyzed directly with the SEM-EDX. Nanoparticle morphology was determined by transmission electron microscopy (TEM) (TEM; CM-100, JEOL, USA at 80 kV). X-Ray

diffraction was used to measure the bagged material phase analysis for both cement types using step width 0.0167° from 5° to 70° and time per step of 59.65s (Panalytical X'pert Pro MPD, Malvern Panalytical, Malvern, United Kingdom).

Table1: Nanoparticles instruments and analytical techniques

Instrument		**Technique**	**Sensitivity**
Scanning mobility particle sizer	SMPS	Charge particle	11 to 1,083 nm
Portable aerosol spectrometer	PAS	Light scattering	250 to 32,000 nm
DISC mini	DISC mini	Diffusion charge particle	10 to 700 nm
Impactor	Marple	Gravimetric	0.52 to 21.3 µm
Inhalable sampler	IOM	Gravimetric	50% Cut-point: 100 µm (Sampling flow rate 2.0 l/min)
Plastic cyclone (Higgins-Dewell)	Cyclone	Gravimetric	50% Cut-point: 4 µm (Sampling flow rate 2.2 l/min)
Transmission electron microscope	TEM	Transmission electron	< 1 nm
Infrared absorption spectrophotometry	IR	Infrared absorption spectrophotometry	Limit of detection (LOD) 5µg/sample
Scanning electron microscope energy dispersive X-ray spectroscopy	SEM-EDX	Scanning electron	± 1%
X-ray diffraction	XRD	X-ray diffraction	± 0.1%

Characterization of the collected airborne particles

Aerodynamic mass particle size distributions from 0.52 to 21.30 µm were measured with an 8-stage cascade impactor (Marple; Thermo Fisher Scientific, Air Quality Instruments, Franklin, MA, USA.). Inhalable fraction (50% Cut-point: 100 µm) was measured with an IOM cassette fitted with a 25 mm PVC filter and a personal pump operating at a flowrate of 2 L/min (IOM and PVC filter; SKC Inc., Eighty Four, PA, USA). Respirable fraction (50% Cut-point: 4 µm) was measured with a plastic cyclone (Higgins-Dewell) (Casella US, Buffalo, NY, USA) operating at a flow rate of 2.2 L/min and equipped with a 37 mm PVC filter (PVC filter; SKC Inc., Eighty Four, PA, USA) as described in NIOSH method 0600 (NIOSH, 1998). Crystalline silica was determined using infrared absorption spectrophotometry (IR; IRAffinity-1S1, Shimadzu, Kyoto, Japan) as described in NIOSH method 7602 (NIOSH, 2003). SEM-EDX analyzes were performed after removing the airborne particles from the IOM filter. We extracted the deposited particles on the filter using carbon adhesive disc stickers (12 mm diameter, Plano GmbH, Wetzlar Germany). Airborne nanoparticles were collected onto the TEM grid (TEM grid; Quantifoil R1/4, Quantifoil Micro Tools GmbH, Germany) using a particle mini sampler (MPS) with a sampling flowrate of 0.3 L/min (MPS; Ecomesure, Sacly, France).

Airborne particle concentration calculations

Particle concentrations were calculated according to NIOSH method 0500 for gravimetric filters.

Particle concentration (mg/m^3) = $[(W_2 – W_1) – (B_2 – B_1)] \times 10^3 / V$

Where: W_1 = Pre-weight of sampling (mg)

W_2 = Post-weight of sampling (mg)

B_1 = Pre-weight of blank (mg)

B_1 = Post-weight s of blank (mg)

V = Air volume sampling (l) or Sampling flowrate (l/min) x time (min)

Work activity simulation experiments

The work activities were simulated in an exposure chamber (2.2m x 2.2m x 2.2m) equipped with a controlled, HEPA-filtered ventilation (class H13 with efficiency 99.5 %, EN 1822) (Guillemin, 1975). Baseline airborne particle concentration in the chamber was sampled after running the ventilation for 2 hours prior to the experiment start. The workers simulating the activity wore a protective chemical suit, respiratory protection (N100, P3, or FFP3), nitrile gloves, goggles, and safety shoes (Figure 1). The ventilation was not operating during the work activity. Ventilation was turned back on and running while the measurements inside the exposure chamber continued for 2 hours after the work activity had finished.

Each of the three simulated activities; bag emptying, concrete cutting, and sweeping were performed in triplicates i.e., three different workers simulated the same task in separate experiments to address potential between-worker differences. **Bag emptying** was performed by cutting open a 25-kg cement bag, and then turning the bag upside-down to pour the cement into a vat on the floor. At the end, the bag was shaken until completely empty as shown in Figure 1A. We made blocks (size 25 x 36 x 6 cm) of concrete (cement and sand mixture) as well as cement blocks without sand. The **concrete block cutting** activity was performed with a circular saw (grinding disc diameter 230 mm and maximum rated speed 6,600 round per minute (RPM) (PWS 20-230 J, BOSCH, Leinfelden-Echterdingen, Germany). We used this saw to cut the blocks for 10 seconds in each experiment as shown in Figure 1B. The **sweeping** activity was performed after pouring one kilogram of cement on the floor, and then sweeping using an ordinary broom. The sweeping activity continued for 1 minute in each experiment as shown in Figure 1C.

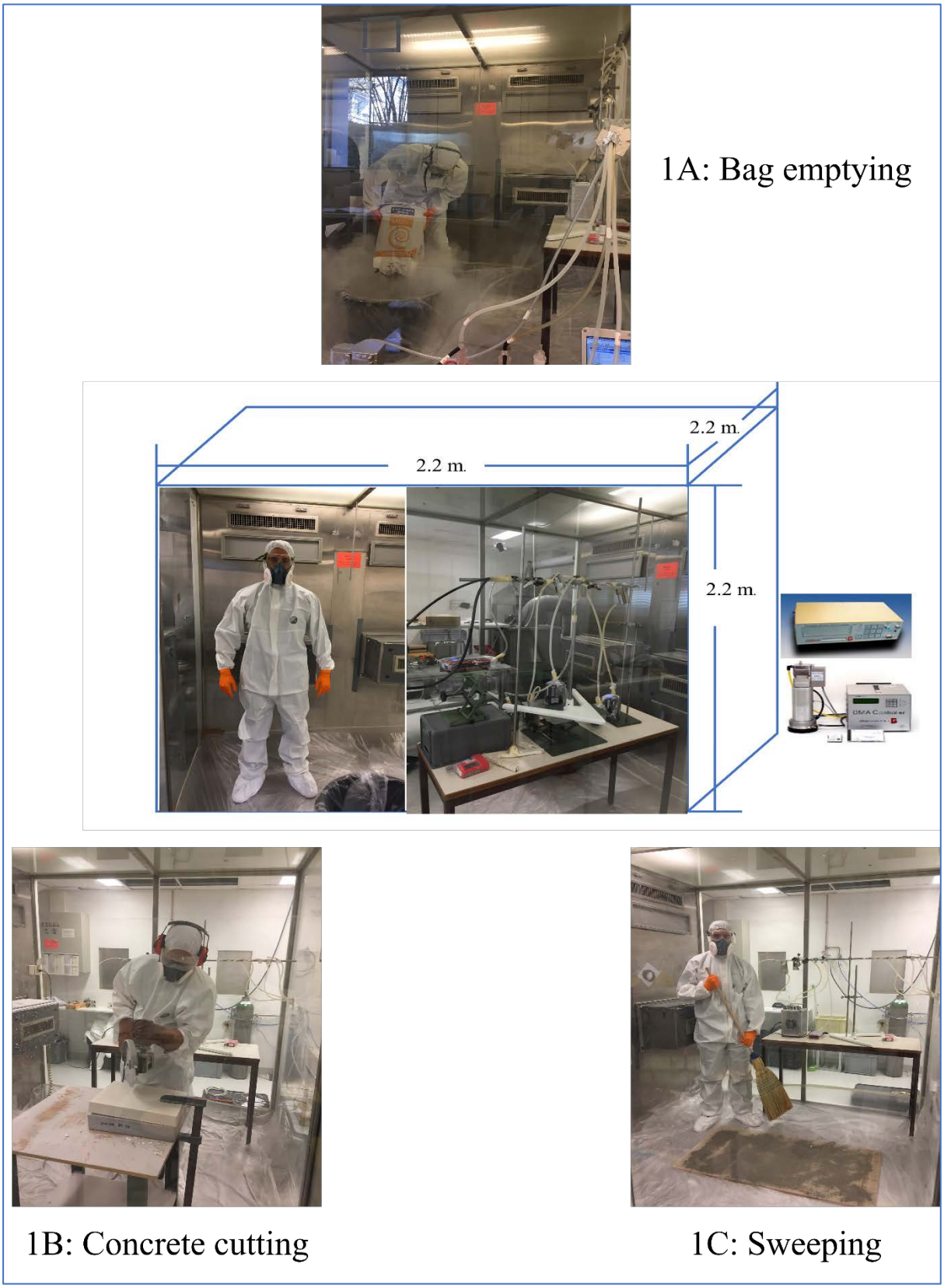

Figure 1: **Experimental setting:** Three working activities such as bag emptying (1A), concrete cutting (1B) and sweeping (1C) in the chamber size: 2.2 x 2.2 x 2.2 meters. Workers wear whole body protection with personal protective equipment (PPE) as following; dust protection cloth, rubber gloves, goggles, safety shoes, and respirator.

Field sampling approach

Company description, Switzerland

In Switzerland, two construction companies and 15 workers were recruited. A convenience sampling approach was used by contacting companies using cement that had previously been sampled for other hazards. One company was housed in a two-story building partially open and no windows. In a large open hall (80 m x 25 m x 10 m), workers constructed large reinforced concrete walls (size ranged from 3 - 5m tall x 1- 3 m long x 0.3 - 0.7 m thick). A cement mixing truck filled an overhead concrete hopper connected to a crane. The crane operator moved the hopper to different workstations using a control panel. The wet concrete was poured into steel molds (Figure 2A). Workers in this area would wire steel rods, build and remove steel molds or wooden frames (Figure 2B). Once the concrete had dried, workers moved the blocks to the polishing station. The polishing workers used hand-held sanding machines on horizontally mounted walls standing on a ladder, or vertical walls laying on a bench (Figure 2C). These pre-manufactured reinforced concrete walls were then loaded onto a truck aimed for the construction site. We sampled workers at the second construction company during work at a building repair site. The workers worked indoors and in pairs. One worker drilled into the concrete wall to remove parts of it using a handheld hammer drill. The second worker held a vacuum cleaner nozzle close to the drill bit to remove dust particles as they were generated (Figure 2D).

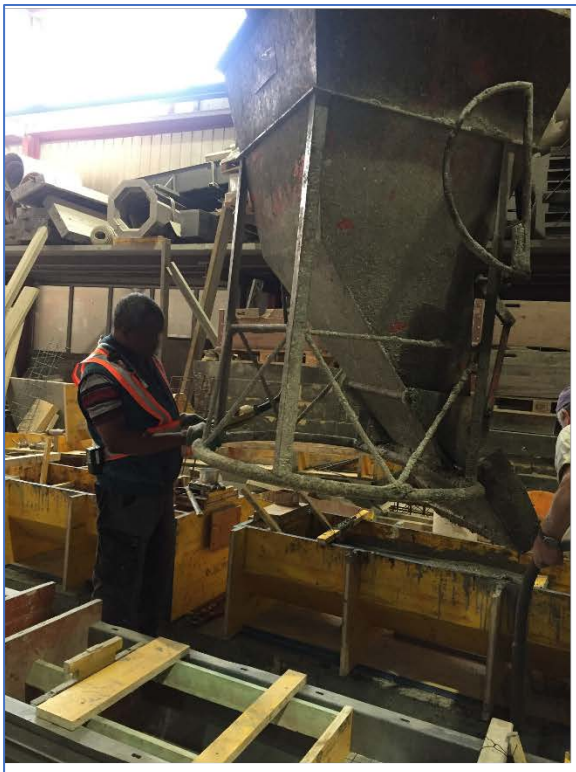

2A: Cement mixing

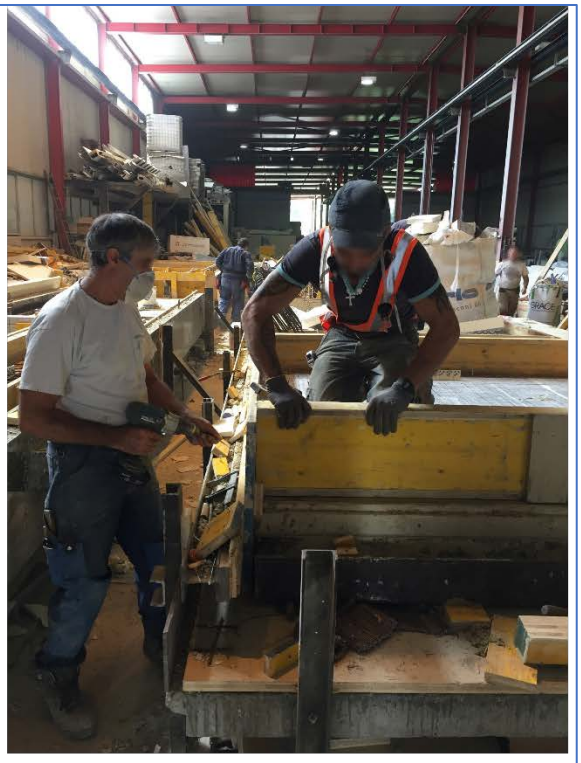

2B: Wooden and wire steel work

2C: Polishing

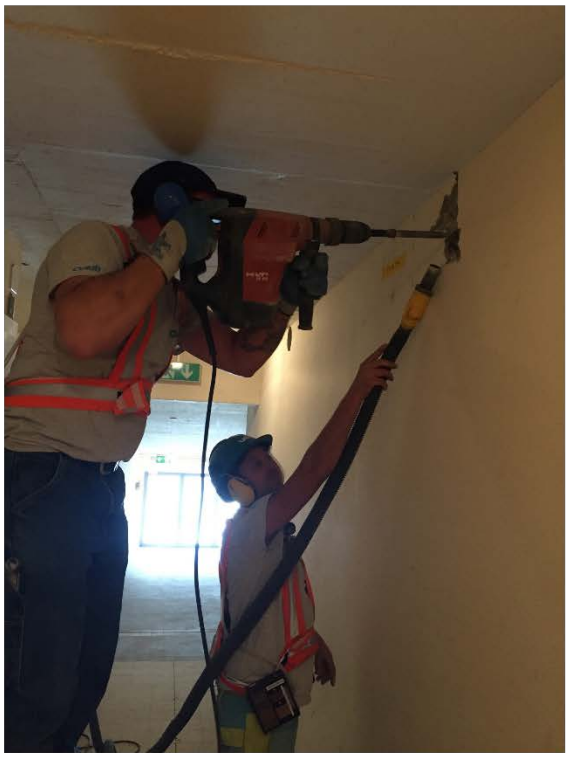

2D: Drilling

Figure 2: Construction working activities in Switzerland

Personal air sampling, Switzerland

Each worker carried a personal sampling train equipped with an IOM inhalable particle sampler (n=15) and a cyclone (n=15), and a DiSCmini (n=15) while performing a specific work activity. Area air concentrations were sampled with SMPS, PAS, DiSCmini, and an impactor. Sampling times were about 2 hours.

Company description, Thailand

In Thailand, 40 workers were recruited from three construction companies. The companies and their workers were recruited while working on the Suranaree University of Technology campus. All companies constructed new buildings such as hospitals, laboratories, and dormitories. Cement mixing was manual (Figure 3A) and semi-automatic (Figure 3B). Workers loaded the vat or cement mixer by cutting open a 25-kg cement bag, pouring, and shaking it until empty. Workers added sand and water to the cement and in manual mixing, used a hoe to mix the wet concrete in the vat. At the end of the task, workers swept the spilled dry cement with a broom (Figure 3C). Sometimes the workers wet-sprayed the cement before sweeping to prevent dust-formation and sometimes they did not. Sweeping and cement mixing were performed inside and outside of the unfinished building. Small hand-held hammer drills were used inside the building to fit electrical wiring (Figure 3D).

Personal air sampling, Thailand

Each worker was equipped with three personal sampling trains: an IOM cassette (n=10), a cyclone (n=10) and an impactor (n=3). No stationary nano sampling instruments were readily available in Thailand, and we could not ship them from Switzerland as the SMPS has a radioactive source. Consequently, no direct-reading instruments were used during the Thai sampling campaigns. Sampling times were about 2 hours per worker.

3A: Manual cement mixing

3B: Semi-automatic mixing

3C: Sweeping

3D: Drilling

Figure 3: Construction working activities in Thailand

Statistical analysis

Descriptive statistical analyses such as geometric mean diameter (GMD) and geometric standard deviation (GSD) were calculated using Excel. Descriptive statistical analyses for particle number and mass concentration were mean and SD, and were calculated using the software integrated in the direct reading instruments.

3. Result

Cement bag emptying

Particle number concentrations during activity and post-activity were similar for the two cement types. For photocatalytic cement, bag emptying generated 3.7 x 10^3 particles per cubic centimeter (pt/cm^3) giving a GMD of 322 nm and a GSD of 2.90; and 3.6 x 10^3 pt/cm^3, GMD 227 nm and GSD 3.31 for regular cement. Figure 4A shows nanoparticle number concentrations and size distributions for both photocatalytic and regular cement during bag emptying measured with the SMPS. Cement bag emptying generated higher particle number concentrations for regular compared to photocatalytic cement in the size range from 11 to 241 nm. Above 241 nm, the number concentrations for photocatalytic cement were higher. Both cement types had a single peak at 692 nm: the modal values were 3.2 x 10^3 pt/cm^3 for photocatalytic and 1.4 x 10^3 pt/cm^3 for regular cement (Figure 4A).

Particles with sizes from 1,083 nm to 32,000 nm were measured with PAS (Figure 4B). Photocatalytic cement had a higher number concentration than regular cement across the entire size range. Irrespective of cement type, 99% of the cumulative airborne particle number during bag emptying was in the size range below 3.5 µm.

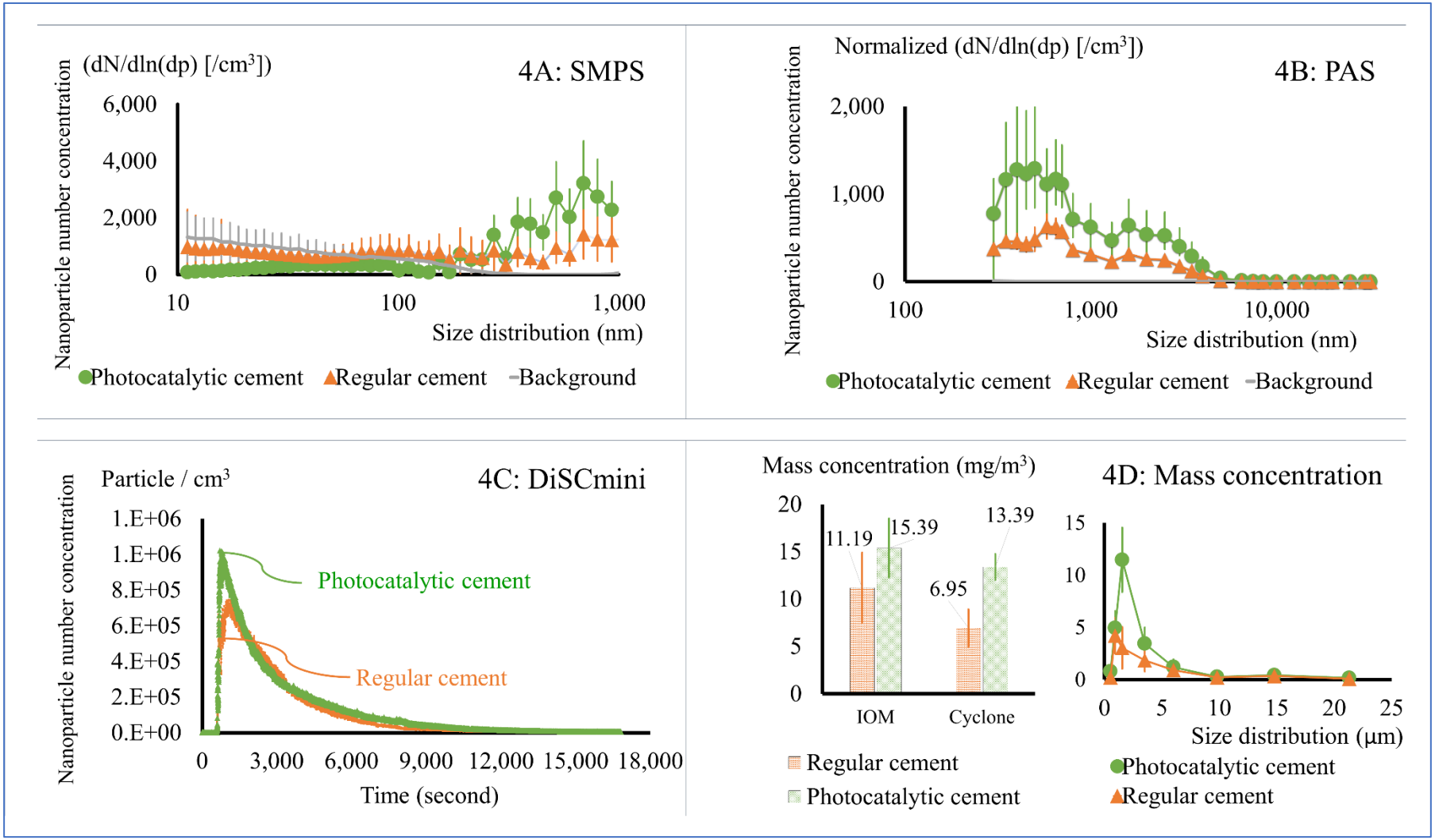

Figure 4: **Bag emptying**: nanoparticle mass and number size distributions and concentrations for photocatalytic cement (solid circles) and regular cement (solid triangle)

Peak concentrations during the bag emptying measured with DiSCmini was approximately 1.0 x 10^6 pt/cm^3 for photocatalytic cement and somewhat lower for regular cement (7.7 x 10^5 pt/cm^3) (Figure 4C). In the DiSCmini's most accurate size range (10-300 nm), the photocatalytic cement GMD was 37 nm, while that of regular cement was 40 nm.

Figure 4D shows the particle mass fractions and concentrations during bag emptying. Inhalable dust mass concentration (measured as inhalable dust) was 15.16 (SD±3.12) mg/m^3 and respirable dust (cyclone) was 13.34 (SD±1.36) mg/m^3 for photocatalytic cement. Inhalable and respirable dust mass concentrations were ~31% and ~49% lower for regular cement, respectively during bag emptying with 10.74 (SD±3.70) mg/m^3 for inhalable dust and 6.75 (SD±1.97) mg/m^3 for respirable dust. Mass particles size distribution showed a peak concentration of 10.67 (SD±5.09) mg/m^3 at 1.55 µm for photocatalytic cement. Regular cement had half the mass concentration (3.99 mg/m^3 SD±1.70) compared to photocatalytic cement and at a smaller size (0.93 µm) as shown in figure 4D.

Airborne photocatalytic cement particles were both nanoparticles and fine particles as observed with the TEM images (Figure 5A and Figure 5B). Regular cement particles are shown in Figure 5C and Figure 5D. The particle boundary layer showed a much greater number of small particles (size around 50 nm) for photocatalytic cement (Figure 5A and Figure 5B) compared to regular cement (Figure 5C and Figure 5D). The presence of nano-sized spherical particles was only found in the photocatalytic cement and might be attributed to nano TiO_2 (Figure 5B). Our measuring device did not have the spatial resolution to determine the elemental composition of the nanoscale particulates; however, we analyzed the chemical composition of the aerosol samples collected during cement working activities with SEM-EDX, and confirmed that these were indeed TiO2 nanoparticles. The regular cement contained mostly coarse

particles. Note that the SMPS reported a smaller GMD than what we observed in the TEM, which were mostly particles around 1 µm, as shown in figure 5C and figure 5D.

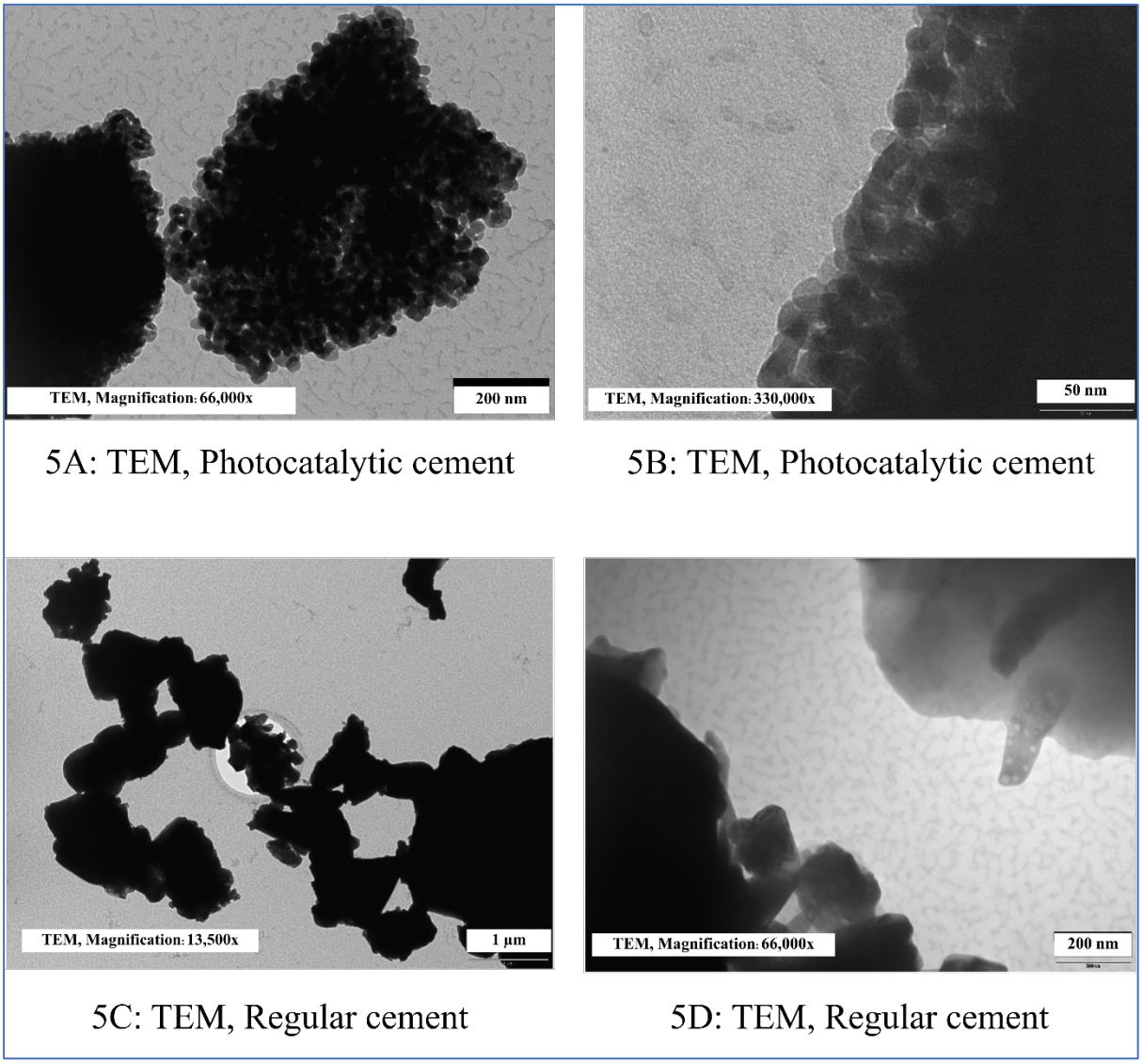

Figure 5: **Bag emptying:** particles morphology between photocatalytic and regular cement

Concrete block cutting

Mean particle number concentration during cutting concrete blocks made with photocatalytic cement was 1.0 x 10^4 pt/cm^3, GMD of 287 nm and GSD of 2.22. Cutting blocks made with regular cement gave 1.9 x 10^4 pt/cm^3, GMD 345 nm and GSD 1.96. Figure 6A shows the nanoparticle size distributions and concentrations for both photocatalytic and regular concrete block cutting measured with SMPS. The size distributions were similar; increasing at particle size 137.8 and fluctuating between 277.8 and 930.5 nm. The peak number concentration was about double for regular cement (1.2 x 10^4 pt/cm^3) at 348.9 nm compared to the peak for photocatalytic cement (5.8 x 10^3 pt/cm^3) at 271.8 nm.

The particle size number distributions measured with PAS were similar for both cement types, except for particle sizes between 300 and 500 nm where regular cement had a greater number concentration than photocatalytic cement. Irrespective of cement type, concrete cutting had 99% of cumulative airborne particle number in sizes below 3.5 µm (Figure 6B).

Figure 6C shows particle number concentrations measured with DiSCmini during concrete cutting. The particle counts were extremely high for both cement types. Photocatalytic cement had peak concentration around 9 million pt/cm^3 while regular cement had a peak at 6 million pt/cm^3. The corresponding GMDs reported by the DiSCmini were 31 nm and 42 nm, respectively.

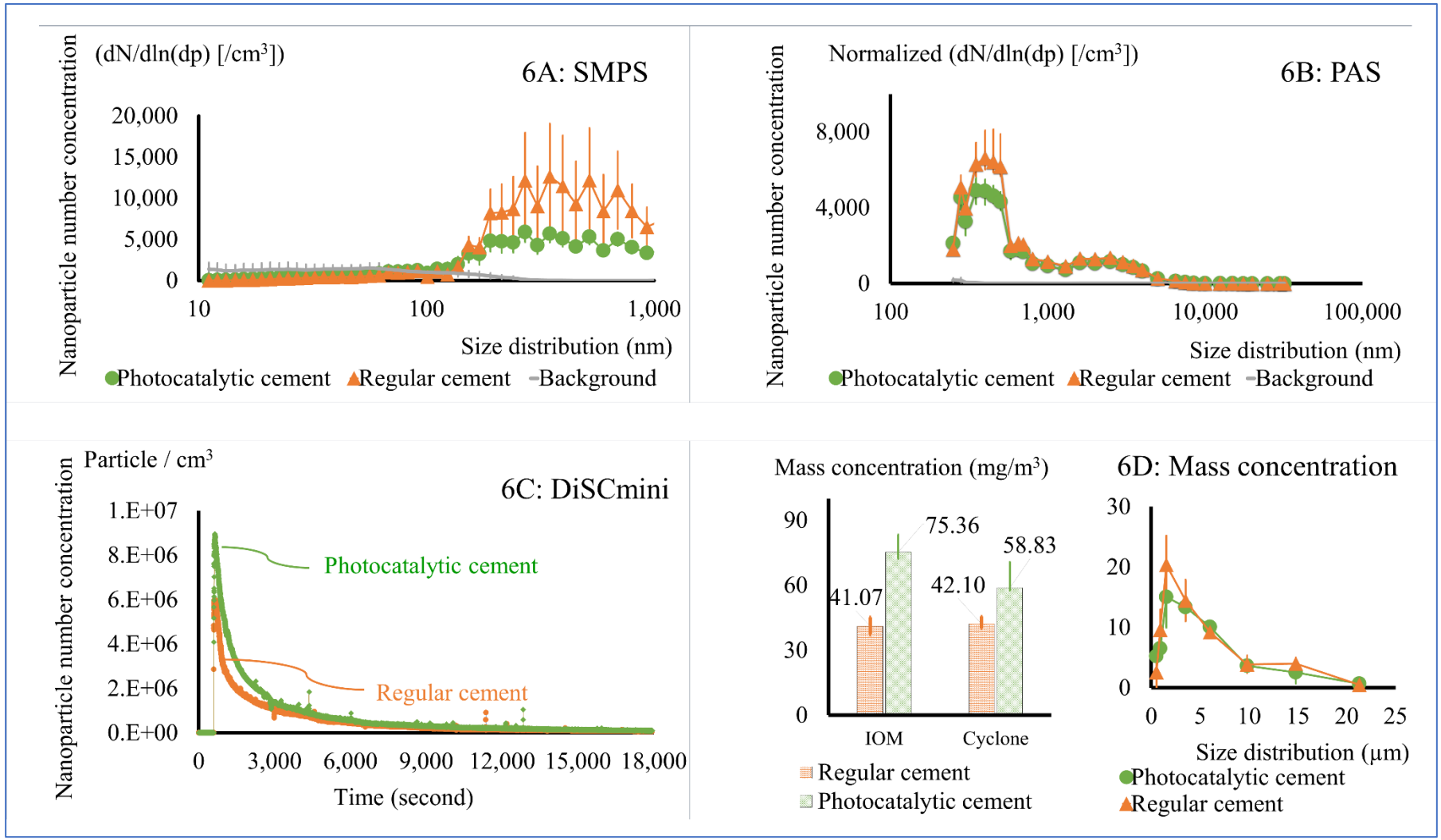

Figure 6: **Concrete block cutting:** nanoparticle mass and number size distributions and concentrations for photocatalytic cement (solid circles) and regular cement (solid triangle)

Inhalable photocatalytic concrete dust mass concentrations during cutting were almost double (75.10 mg/m^3, SD±7.92) compared to regular cement (40.95 mg/m^3, SD± 4.16) with a ratio of photocatalytic to regular cement of 1.8. Respirable dust concentrations generated during concrete cutting were somewhat similar for photocatalytic cement (57.99 mg/m^3, SD± 11.96) and regular cement (42.01 mg/m^3, SD± 3.52) with a ratio of photocatalytic to regular cement of 1.4. Cutting photocatalytic and regular cement concrete had the same peak mass concentrations at 1.55 µm mean size and airborne concentrations of 19.90 (SD± 5.06) and 14.54 (SD±4.79) mg/m^3, respectively (figure 6D).

Figure 7 displays particle morphology images for airborne photocatalytic (Figure 7A and Figure 7B) and regular (Figure 7C and Figure 7D) cement sampled with a TEM grid during cutting. The morphology for fine particles generated during concrete cutting was similar for the two cement types. The presence of nano TiO_2 spherical particles was not observed for photocatalytic cement concrete cutting.

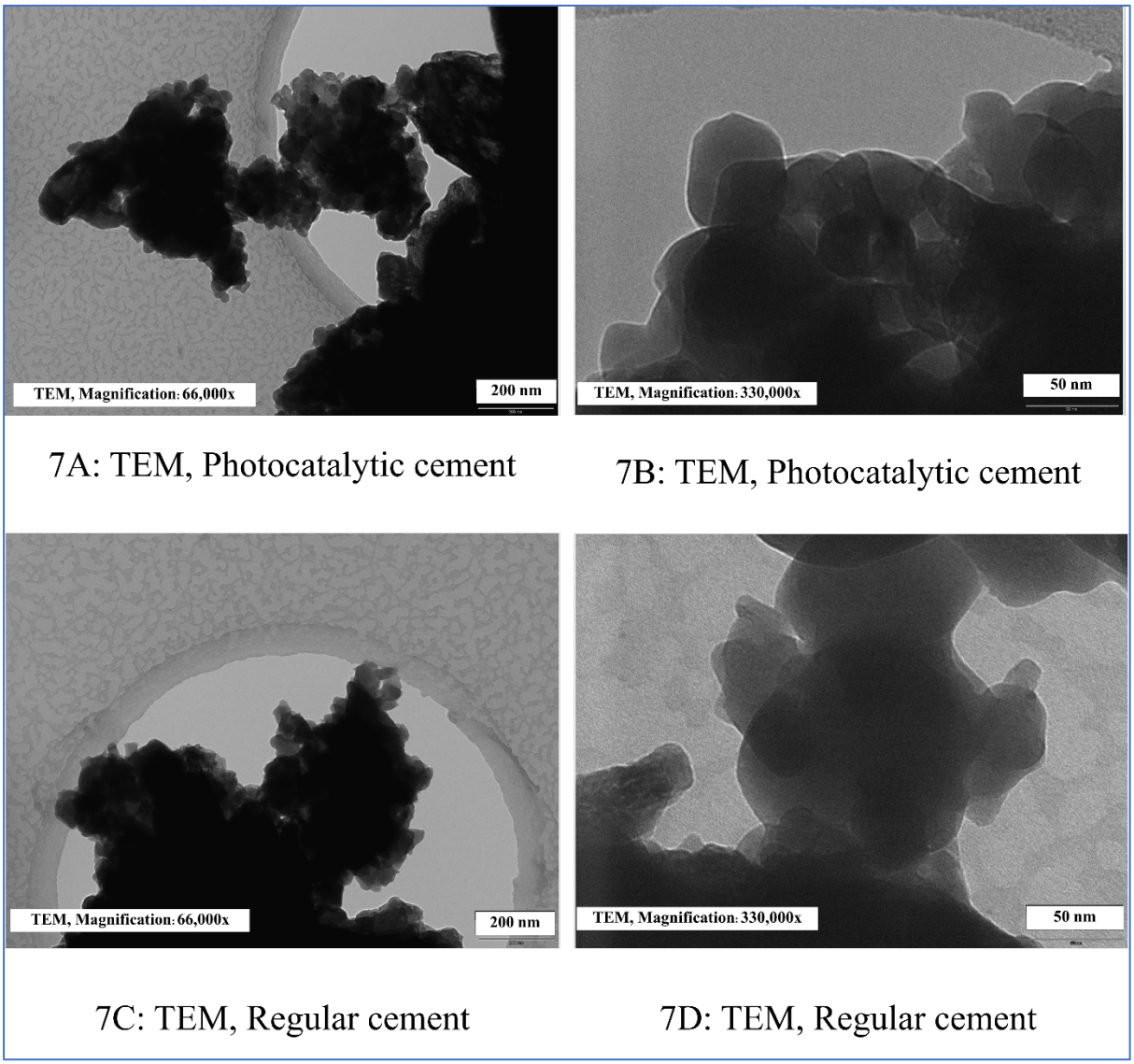

Figure 7: **Concrete cutting**: particles morphology between photocatalytic and regular cement

Cement sweeping

Nanoparticle size number distributions and number concentrations measured during sweeping with SMPS showed photocatalytic cement mean particle number concentrations of 1.8 x 10^3 pt/cm^3, GMD of 194 nm and GSD of 3. The same particle number concentrations (2.2 x 10^3 pt/cm^3) was observed for regular cement but for larger particles (GMD 283 nm and GSD 3) (Figure 8A). Sweeping had a particles peak size of 692 nm with number concentrations double for photocatalytic (1.0 x 10^3 pt/cm^3) compared to regular (5.1 x 10^2 pt/cm^3) cement.

Figure 8B shows particle size number distributions and number concentrations for particles between 250 and 32,000 nm. Again, sweeping had a greater particle number concentration for photocatalytic cement compared to regular cement.

Photocatalytic cement had a peak concentration around 9.3 x 10^5 pt/cm^3 while regular cement had a peak at 8.3 x 10^5 pt/cm^3 (Figure 8C) measured with DiSCmini during cement sweeping.

Mass particle size distributions and concentrations for photocatalytic and regular cement during sweeping measured with three different personal air instruments (IOM filter cassette, cyclone and impactor) are shown in Figure 8D. Inhalable dust concentrations were 30% greater (15.19 (SD± 2.35) mg/m^3 for photocatalytic compared to regular cement (10.53 (SD± 1.60) mg/m^3). Respirable dust concentrations for photocatalytic cement were about double the concentration (9.52 (SD± 2.99) mg/m^3) of regular cement (4.98 (SD± 1.98) mg/m^3). Photocatalytic and regular cement during sweeping had the same peak at 1.55 µm with 5.26 (SD± 2.33) and 3.86 (SD±1.47) mg/m^3, respectively.

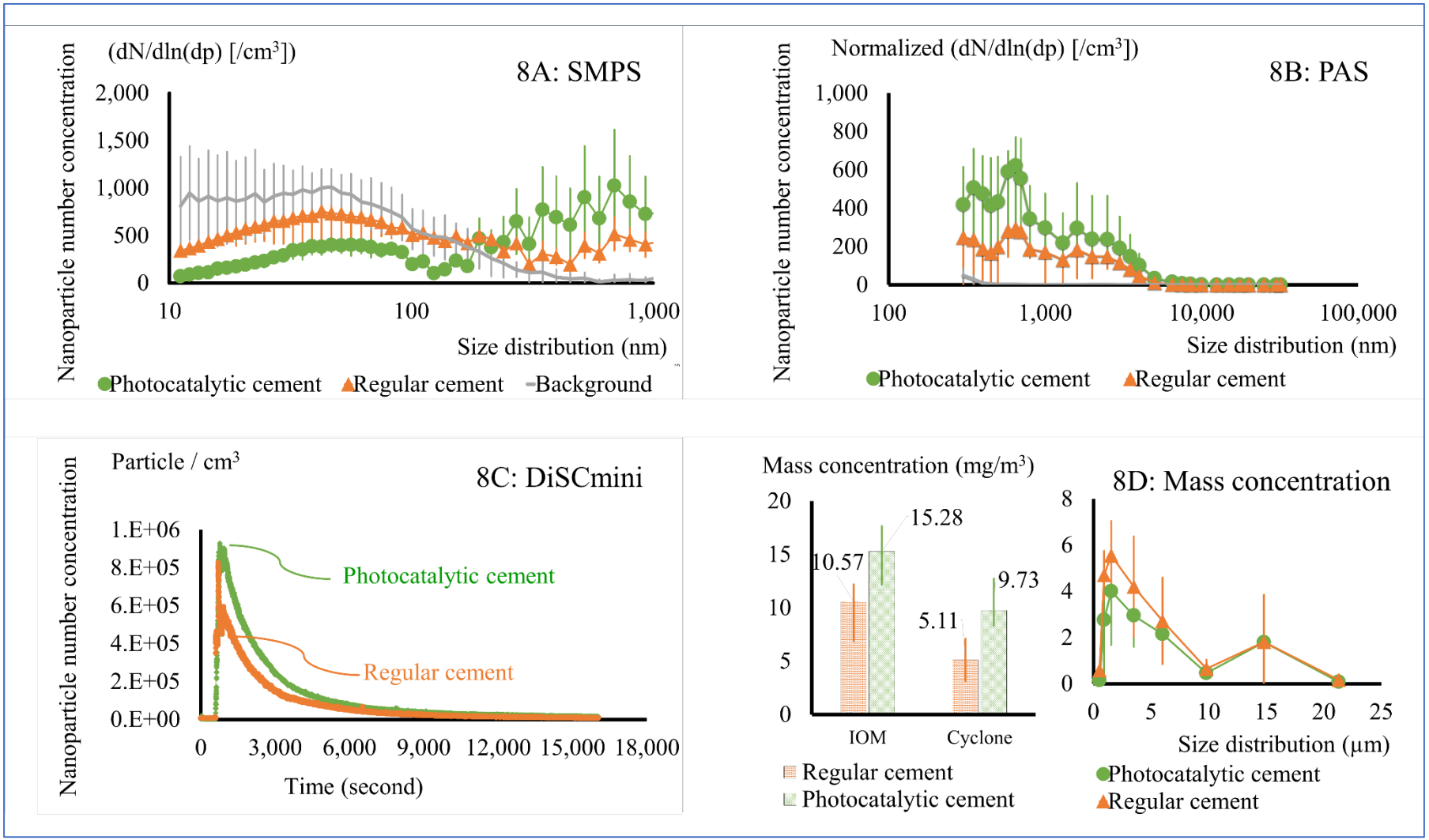

Figure 8: **Sweeping:** nanoparticle mass and number size distributions and concentrations for photocatalytic cement (solid circles) and regular cement (solid triangle)

Airborne photocatalytic cement contained two distinct types of nanoparticles as well as coarse particles (Figure 9A and 9B). The presence of nano-ranged spherical particles was only observed for photocatalytic cement and we attribute this to the presence of nano TiO_2 (Figure 9A and 9B). The regular cement contained mostly coarse particles (particles size around 1 µm) as shown in figure 9C and 9D.

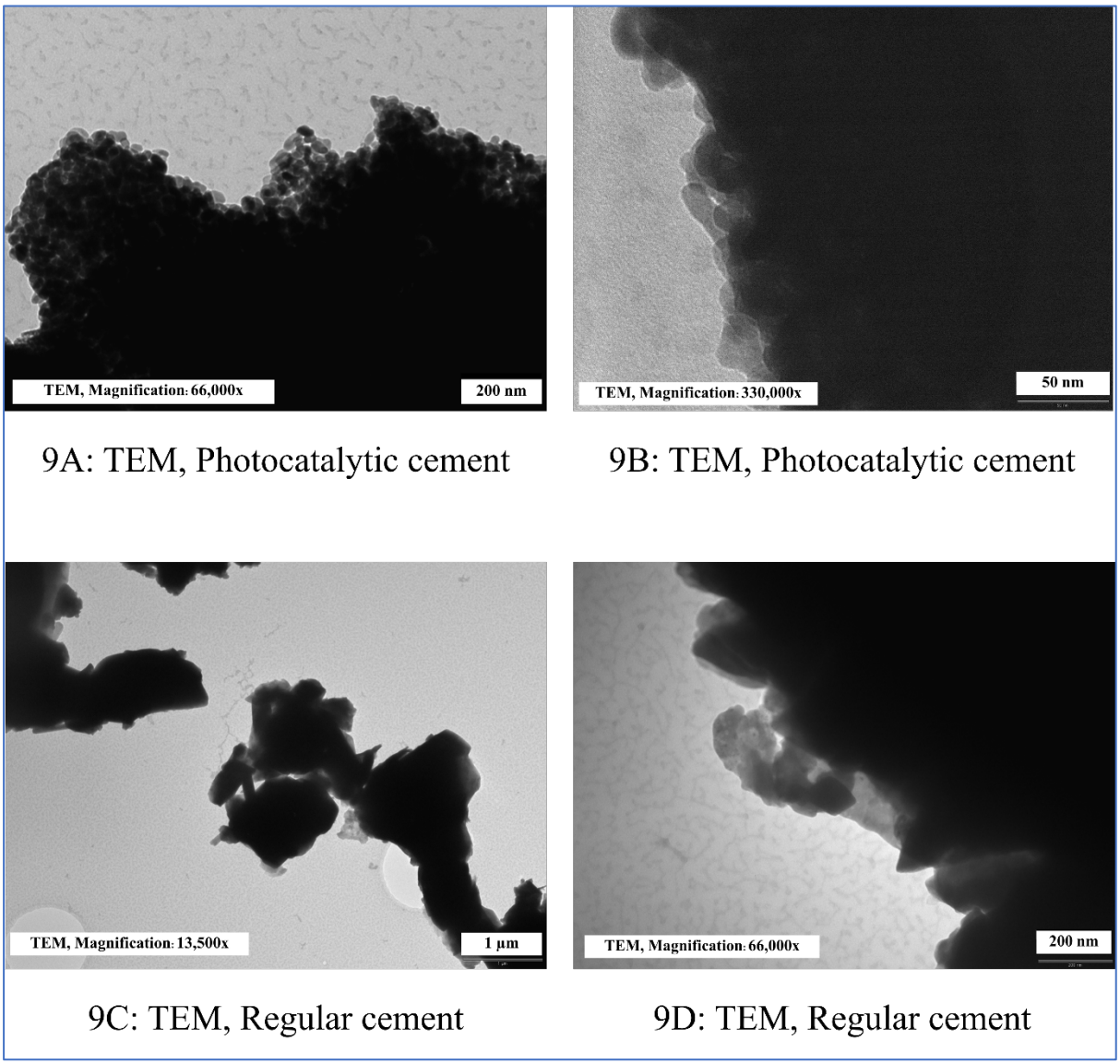

Figure 9: **Sweeping:** particles morphology between photocatalytic and regular cement

Elemental composition analysis

Elemental compositions were analyzed by SEM-EDX and the results for both cement types by working activities are shown in Figure 10. Calcium oxides (assumed to be CaO) and silicon dioxides (assumed to be SiO_2) were the elemental substances detected in greatest quantity. Photocatalytic cement (bag sample) contained around 2 wt% nano TiO_2. This assumes that the information from the photocatalytic cement manufacturer was true that they added nanoTiO_2 (percent nanoTiO_2 was not given). The components were then defined based on what is known about the various oxides expected in cement. As nanoscale particles contained Ti and O in the expected ratio of approximately 1:2, it is sound to assume that these are TiO_2 nanoparticles. Furthermore, the TEM image from the bag emptying showed the presence of nanosized particles for photocatalytic cement but not for regular cement, and finally, the SMPS measurements showed nanosized particle fraction for bag emptying at 17%. Regular cement (bag sample) contained no detectable nano TiO_2. Photocatalytic cement bag emptying and sweeping had the highest airborne nano TiO_2 concentration 16.5 wt% (GSD±1.72) and 9.7 wt% (GSD±1.36), respectively. Photocatalytic cement concrete cutting contained 2.0 wt % nano TiO_2, which was the same concentration found in the bag sample. None of the airborne aerosol samples collected during activities with regular cement contained nano TiO_2. The mass concentration of nano TiO_2 in photocatalytic cement was calculated from element composition and inhalable dust mass concentration (sampled on the filter). Our work activity simulation showed airborne TiO_2 mass concentrations for photocatalytic cement bag emptying 2.50 mg/m^3, concrete cutting 1.53 mg/m^3, and sweeping 1.48 mg/m^3, respectively, for particles size >100 nm.

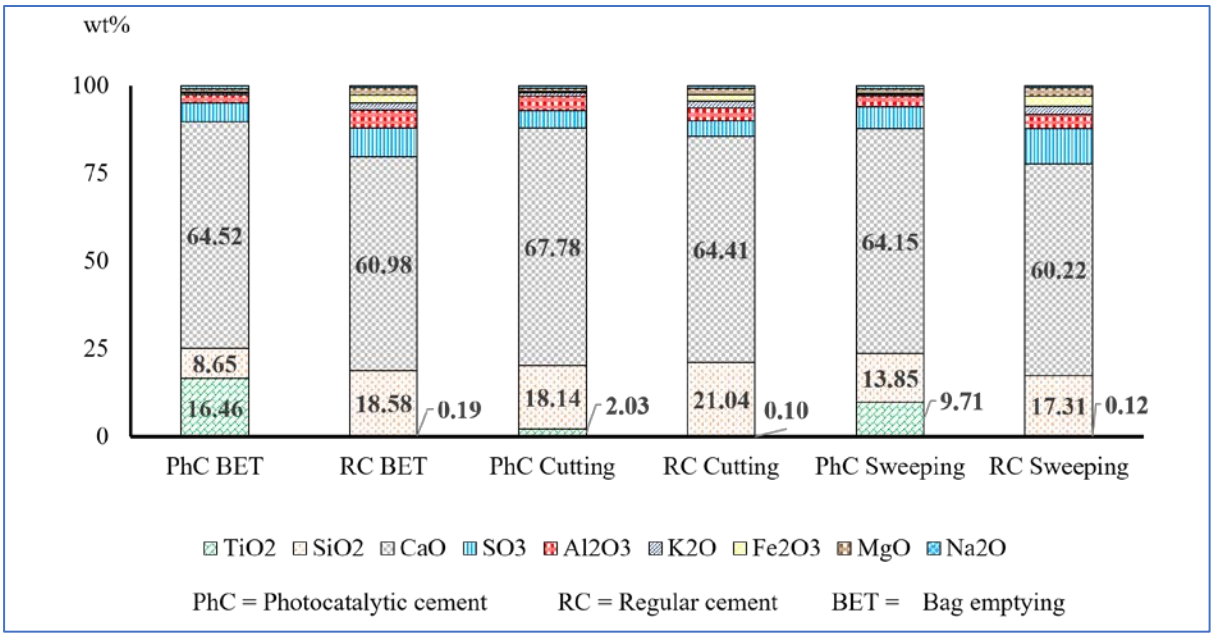

Figure 10: Elemental composition analysis from (SEM-EDX) given in percent for each substance from cement working activities

Cement powder samples were analyzed with X-ray diffraction and the phase analyses are shown in Table 2. Tricalcium silicate (Ca_3SiO_5) and dicalcium silicate (Ca_2SiO_4) were the most abundant elements in both cement types. Photocatalytic cement contained 2.6 wt% of nano TiO_2 in two different forms: anatase (1.8 wt%) and rutile (0.8 wt%).

Table2: Cement powder phase analysis by X-ray diffraction

Mineral	Chemical formula	Bulk material (wt%)	
		Photocatalytic Cement	Regular Cement
Tricalcium silicate (alite)	Ca_3SiO_5	61.4	58.2
Dicalcium silicate (belite)	Ca_2SiO_4	14.2	15.6
Tricalcium aluminate	$Ca_3Al_2O_4$	2.3	6.9
Tetracalcium aluminoferrite	$Ca_4Al_nFe_{2-n}O_7$	3.4	5.7
Calcite	CaCO3	10.1	7.9
Anhydrite	$CaCO_3$	2.5	2.7
Gypsum	$CaSO.\ 2H_2O$	1.4	1.1
Portlandite	$Ca(OH)_2$	1.3	1
Lime	CaO	0.5	0.7
Quartz	SiO_2	0.3	0.2
Titanium dioxide	TiO_2		
• Anatase		1.80	0.00
• Rutile		0.80	0.00

We found crystalline silica only during concrete (cement + sand) cutting for photocatalytic and regular cement with the following concentrations 2.5 and 3.5 mg/m^3, respectively. When only cement was used (no sand), the crystalline silica concentrations were always below the detection limit (LOD = 5 μg / sample).

Field sampling at the construction sites

During our study, we discovered that authorities in both Switzerland and Thailand discourage the use of photocatalytic cement due to the lack of information related to health effects associated with this exposure. The photocatalytic cement is already on the European and US market, but we were unable to find the amounts sold per year. We were thus not able to give an estimate for the number of workers potentially exposed, or to identify companies that use these

products. Consequently, we collected samples in the construction industry among workers using only regular cement.

We collected the Swiss samples from July to September. The temperatures ranged during collection from 20 °C to 25 °C, and relative humidity was 50-60%. We sampled the Thai workers from November to December, and the temperatures were between 30-35 °C, and the relative humidity was 60-70%.

GMs and GSDs for size number distributions and number concentrations obtained at the Swiss construction sites are shown in figure 11A and 11B. Mean airborne particle number concentrations over 2 hours was 46,000 pt/cm^3, GMD was 49 nm and GSD was 2.4. Peak nanoparticle concentrations measured with the DiSCmini were for construction (n=5) 4.9 x 10^5 pt/cm^3. Polishing (n= 5) was double (9.9 x 10^5 pt/cm^3), and drilling activity (n=5) was slightly above (6.5 x 10^5 pt/cm^3). Figure 11C shows peak nanoparticle concentrations for the three activities separately in the same graph.

The mean mass concentration for inhalable dust was more than threefold greater for Switzerland (7.08 mg/m^3, SD±3.02) compared to Thailand (2.22 mg/m^3, SD±1.61) (Figure 11D). This was also true for respirable dust (Switzerland had 4.00 mg/m^3, SD±2.31 and Thailand 1.19 mg/m^3, SD±1.15).

Mass particle size distributions (Figure 11D) were quite different between the two country-specific construction sites. The Swiss construction site had a peak mass concentration of 2.22 mg/m^3 (SD±0.61) at 1.55 µm, while in Thailand the peak was just a fraction of this (0.57 mg/m^3 SD±0.46) and for smaller particles (0.93 µm).

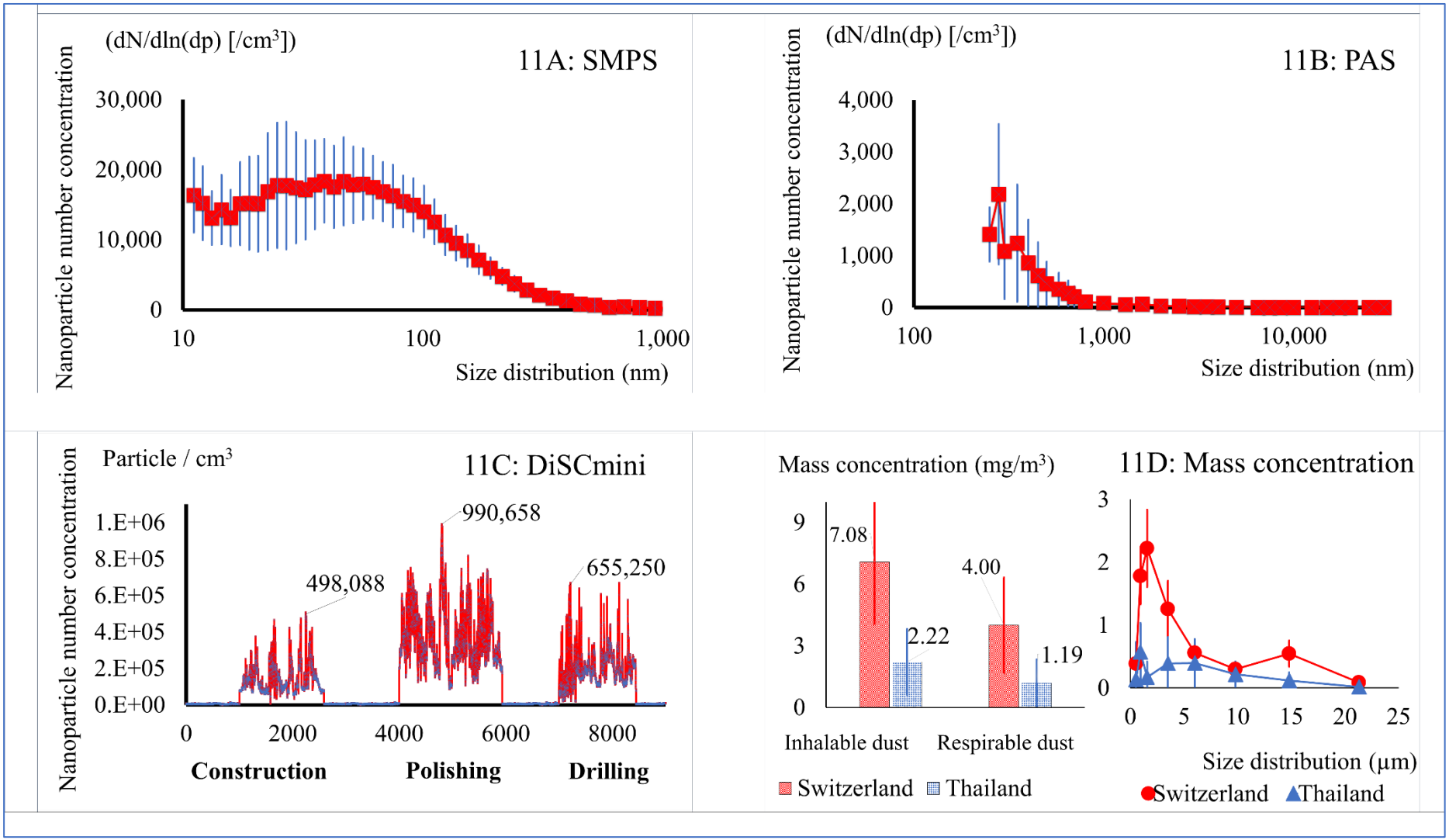

Figure 11: **Construction sampling:** nanoparticle mass and number size distributions and concentrations in construction

4. Discussion

In experiments with photocatalytic cement, we observed much larger mass-fractions of airborne particle-bound TiO_2 during sweeping (9.7 wt%) and during bag emptying (16.5 wt%) than what we found in the bagged cement (2 wt%). This shows that nano TiO_2 was easily airborne during activities with cement powder. It is in agreement with our previous dustiness study conducted with the same cement type where we observed nano TiO_2 to become airborne far easier than the remainder of the cement powder (Batsungnoen et al., 2019). Both nano TiO_2 crystalline phases, anatase and rutile, were identified in the photocatalytic cement (Table 2). It is important to understand what proportion of the nanomaterial additive that is airborne when assessing workers' exposures to nano cement. We analyzed the cement powder sampled directly from the bag shipped by the manufacturer with XRD. We characterized the composition of both the photocatalytic and the regular cement powders. These results are given in Table 2 and show that photocatalytic cement contained 2.6% TiO2. XRD analysis need a minimum of 3 g of sample. Unfortunately, we cannot analyze the dust collected with air sampling with XRD because air samples contain far less than the required amount. Due to this limitation, we confirmed the chemical composition in a few aerosol samples collected during cement working activities with SEM-EDX. We focused on a single dot with a 300 nm dimeter in the SEM-EDX images which showed this particle to be 82% TiO_2.

The work activity and the form in which the nano-additive is present also seem to play an important role. Notably, photocatalytic cement concrete cutting resulted in similar proportions of nano TiO_2 (2 wt%) in airborne nanoparticles as in bagged cement material. This suggests that the nano-additive was well bound to the matrix during the cutting, and consequently, the nano TiO_2 particles were released in the aerosol as a part of the concrete particles. We cannot visualize chemically bound particles, but rely on dispersion as a measure of the degree to which

particles clump together into agglomerates or aggregates. We measured dispersion as the particle size distribution and the width of a particle size distribution. We observed small particles on the boundary of larger particles on the TEM image obtained during bag emptying (Fig. 5) and sweeping (Fig. 9) photocatalytic cement. We did not observe these small particles in the TEM images obtained for the same activities with regular cement. Consequently, we conclude that these smaller particles are mainly TiO_2 nanoparticles as this was the only difference between photocatalytic and regular cement as well as the SEM-EDX analysis. The TiO_2 nanoparticles agglomerated to the larger particle and are held together by weak bonds (e.g., van der Waals forces or physical entanglement). TEM images obtained from air sampling during concrete cutting (Fig. 7) showed only 2% TiO_2. We observed that these particles were embedded in larger concrete particles resembling an aggregate, which are generally held together by covalent bonds. Covalent bonds between TiO_2 and SiO_2, $CaCO_3$ and SO_3, have previously been shown by FTIR analysis (Zouzelka and Rathousky, 2017; Yang et al., 2018). We hypothesize that the nano TiO_2 in the dry cement powder is not chemically bound as we could observe primary nanoparticles in the TEM image for bag-emptying (Figures 5A and 5A) and sweeping (9A and 9B). We believe that nanoparticles were bound to the concrete surface when water was added, as we observed no primary nanoparticles for cutting either for regular or photocatalytic cement (Figure 7).

Inhaling nano TiO_2 has been associated with respiratory problems in animals (Kwon et al., 2012). An association between photocatalytic cement and respiratory problems is not known as no such studies are available. We can hypothesize that an association between photocatalytic cement exposure and respiratory problems is possible given that nano TiO_2 is released from photocatalytic cement. The nano TiO_2 concentrations in our experiments were low (10^3 particles/cm^3 range) compared to the respiratory study in rats that showed nano TiO_2 to be toxic

at particle number concentration in the 10^6 range (Kwon et al., 2012). The study exposed the rats to only nano TiO_2 therefore it is difficult to extrapolate to possible health effects from exposure to a mixture of cement and nano TiO_2 particles. Complexing the matter further, the lung injury induced by nano TiO_2 depended on dimension, size distribution, concentration, crystal phase, agglomeration, surface coating, chemical, and physical properties (Noël et al., 2012; Wang and Fan, 2014).

Both photocatalytic and regular cement had 99 % of the airborne particles with sizes less than 3.5 µm in all working activities; and can thus be deposited and diffuse into the respiratory tract especially in the alveoli (Oberdörster et al., 2005; ICRP, 1994; Sha et al., 2015; Tedja et al., 2011). The mean size of airborne cement particles during simulated working activities was 200-350 nm, which were far greater than what we found at the construction sites (mean size was 49 nm). This was surprising, and possibly not related to the cement but rather to the diesel truck picking up the concrete walls, since diesel operated vehicles often emit particles in the 50 nm size range (Xue et al., 2015).

World-wide, only few occupational exposure limits (OELs) exist for nano TiO_2. The US Occupational Safety and Health Administration (OSHA) and NIOSH recommend a nano TiO_2 exposure limit for 8 hours to be (NIOSH, 2011; OSHA, 2013):

- particle size >100 nm OEL= 2.4 mg/m^3
- particle size <100 nm OEL= 0.3 mg/m^3

In addition, the French Agency for Food, Environmental and Occupational Health & Safety (ANSES) recommends a toxicity reference value (TRV) for inhaled TiO_2 nanoparticles with particle sizes from 25 nm (P25) of 120 mg/m^3 (ANSES, 2019).

Our work activity simulation showed airborne mass concentrations for photocatalytic cement bag emptying (2 min) of 15 mg/m^3 thereof 16.5% TiO_2 (from the elemental composition analysis), which gave 2.5 mg/m^3 TiO_2. Assuming different bag emptying work scenarios and that exposure increased linearly with 2.50 mg/m^3 with each bag emptying. Emptying four consecutive bags would then give a total of 10 mg/m^3 TiO_2 (2.5 mg/m^3 TiO_2 x 4 bags). This averages out over 4 hours to be 2.50 mg/m^3 (10 mg/m^3 TiO_2 / 4 hours). We observed that workers emptied 2-4 bags during the morning as well as the afternoon shifts in Thailand. Thus, workers worked eight hours per day and emptied eight bags per day (four in the morning and four in the afternoon). Emptying eight bags will generate (2.5 TiO_2 mg/m^3/bag x 8 bags) 20 mg/m^3 TiO_2. Averaging this over the workday gives and upper range of 2.5 mg/m^3 TiO_2 (20 mg/m^3 TiO_2 / 8 hours/day). This time weighted average is just above the OEL for particle sizes >100 nm. We compared our results with this OEL since our GM particle size diameter was 322 nm. To reduce the airborne dust concentrations, we could recommend that workers should empty less than 8 bags during a shift, but that would not be cost effective. Another strategy would be to reduce the airborne particles that lingers in the air post-bag emptying as we observed in the simulations (Figure 4C). The workers would empty one bag, add water, and then mix, and repeat this procedure four times. This would bring the dust concentrations down to background within 15 min thus the average over the shift would not exceed 2.5 mg/m^3 TiO_2. Consequently, the morning exposure would be 2.5 mg/m^3 TiO_2 and same in the afternoon, which gives a total exposure of (2.5 mg/m^3 TiO_2 + 2.5 mg/m^3 TiO_2) 5 mg/m^3 TiO_2 per day averaged over 8 hours would be 0.62 mg/m^3 TiO_2 (5 mg/m^3 TiO_2 / 8 hours). These values are based on our exposure chamber simulations and would of course be altered by worksite specific elements such as factors affecting the dispersion like wind and openness of the space as well as factors affecting release and agglomeration such as rain and humidity. In our simulation study, bag emptying generated the greatest amount of airborne nano TiO_2 thus this work

activity is of greatest concern. In Switzerland, cement arrived at the worksite already mixed with water thereby reducing this exposure among construction workers. Another approach would be that the producers develop a formula that would add nano TiO_2 as a liquid dispersion, thereby reducing the potential for aerosolizing these particles.

Cement dust is regulated in Thailand and Switzerland as particulates not otherwise regulated (PNOR). The Thai OEL for PNOR dust is 15 mg/m^3 for inhalable and 5 mg/m^3 for respirable dust. In Switzerland, the OELs are slightly lower; 10 mg/m^3 and 3 mg/m^3 for inhalable and respirable dust, respectively. Thai construction workers were not exposed above the Thai OELs, while the Swiss construction workers were exceeding the Swiss OEL for respirable dust. The jobs performed were similar among the Swiss and Thai construction workers, but the difference was that the Swiss construction workers used powerful machine tools, in particularly during concrete polishing and drilling, while the Thai construction workers worked with small hand-held hammer drills. Power tools have shown to generate more dust compared to manual tools such as drilling concrete, which generated the highest exposures for quartz and respirable dust among construction workers (Deurssen van et al., 2014). Moreover, Qi and colleagues (Qi, Echt, and Gressel, 2017) reported that concentrations of airborne particles during fiber cement cutting increased with the power of the tools used. The main factors associated with particle generation were number of blade teeth, blade rotating speed, and cutting feed rate (Qi, Echt, and Gressel, 2017). We found comparable result in our work activity simulation, where cutting concrete blocks using power tools generated high particle concentrations (Figure 6). We confirmed that calcium dioxides made up 62 wt% of the airborne particles generated during work activity simulation; the same concentration as in cement (Meo, 2004). This was observed irrespective of cement type and working activities. If we assume 62% of the total particle concentration in the Swiss construction (GM 7.08 mg/m^3) as CaO, we get 4.38 mg/m^3 CaO

(7.08 mg/m^3 CaO x 62%). This estimate was twice the Swiss OEL (2 mg/m^3). The Thai OEL for CaO is more than double of the Swiss OEL, i.e., 5 mg/m^3. Performing the same estimate for CaO concentration for the Thai workers (GM 2.22 mg/m^3), gave 1.37 mg/m^3 (2.22 mg/m^3 CaO x 62%), which was below both Swiss and Thai OELs. Although, the Swiss construction workers were below the PNOR OEL, exposure reduction measures are still needed as they exceed the OEL for CaO. Although, both countries' OELs were established to protect against upper respiratory tract inflammation produced by CaO's alkaline properties (TOXNET, 2014; NJDHSS, 2003), the countries' feasibility assessments for respecting the limit resulted in different values.

The second most abundant airborne particles were SiO_2. CaO and SiO_2 were chemically bound to tricalcium silicate (Ca_3SiO_5) and dicalcium silicate (Ca_2SiO_4) in the cement. Although, we quantified 0.2-0.3 wt% crystalline SiO_2 in cement (Table 2), only the respirable fraction of the airborne dust during concrete cutting was present as crystalline SiO_2. Thus, respiratory crystalline SiO_2 originated from the sand and not from the cement as previously reported by others (McLean et al., 2017). The levels of crystalline silica observed were very high, well above the 8-hour OEL levels, which suggests that for dusty work activities with concrete, the greatest risk comes from crystalline silica in sand rather than from nano-additives.

Sweeping with a broom generated inhalable and respirable dust greater than the Swiss and Thai OELs during simulation (Figure 1C, Figure 8) but not in the field (Figure 3C, Figure 11 includes sweeping with other job activities). The field samples were likely lower because the work place was generously ventilated (some jobs were performed outside) while the simulations were performed in an exposure chamber (10 m^3) without ventilation. Although, the simulations were not able to generate field concentrations, it gave us a relative ranking of the

particle exposure that we observed in the field: very high exposure during cutting (41-75 mg/m^3, Figure 6D), and much lower and similar concentrations for bag emptying (11-15 mg/m^3, Figure 4D) and sweeping (11-15 mg/m^3, Figure 8D). Other researchers have also found that sweeping cement is associated with higher airborne particle concentrations (GM 0.79-1.2 mg/m^3) compared to other cement production jobs such as laboratory, foreman and administration (GM 0.42-0.45 mg/m^3) (Notø et al., 2015). In Notø and colleagues's very large study comprising 24 cement plants in eight countries, they found 63% of the variability to be explained by plant differences. This could also be true for the differences in airborne particle concentrations we observed between Switzerland and Thailand; however, due to the limited number of samples in our study, we cannot calculate this. One study specifically reported concentrations during cleaning using brooms at two cement plants in Ethiopia (Zeleke et al., 2011). They confirmed significantly greater exposures to total and respirable dust in these cleaners compared to other production worker at the same plants.

Sweeping photocatalytic cement produced 31% more inhalable airborne particles (Figure 8D) than regular cement. This increase in mass is probably not explained by the slight increase in airborne particles less than 5 µm as this would not significantly add mass. Rather particles around 15 µm would contribute to the increase in mass observed. Why we have a greater mass concentration in photocatalytic cement compared to regular cement, we can only speculate. Perhaps the addition of nano TiO_2 to the cement contributes to agglomeration of particles of smaller size than if absent, thus the particles generated will be airborne over a longer time. We have not found any scientific publications describing or refuting such a postulation.

Cleaning using other methods than a broom would reduce the cement exposures among Thai construction workers, while Swiss construction workers will need other protective measures to reduce exposures. Exposures to airborne cement particles in the construction industry also depends on duration, environment (temperature, humidity and wind), space (indoor, outdoor), workplace sizes, machine tool use, material type, control measures, and use of personal protective equipment (PPE). We observed that Thai construction workers did not use respiratory protective equipment (RPE) while Swiss construction workers did. Thai construction workers were not comfortable using RPE because it was both hot and humid. Control measures need to be implemented for the Swiss construction workers to not only comply with the Swiss OEL regulations, but to reduce the risk of developing COPD. Local exhaust ventilation (LEV) in construction were shown to be effective in reducing respirable dust in both the work and adjacent area (Kokkonen et al., 2019).

The protection measures needed for workers working with photocatalytic cement, especially during dry cement work, should be similar to recommendations made for nano TiO_2 exposures. Wet processes to reduce airborne dust exposures should be recommended if possible. Several international bodies have recommended ways to reduce nano particle exposures using engineering controls such as enclosed process chambers with negative pressure and local exhaust ventilation (LEV) installed with high-efficiency particulate air (HEPA) filters (NIOSH, 2011; NIOSH, 2012; NIOSH, 2013; OSHA, 2013; Goede et al., 2018). Where enclosure of the source is not possible other alternatives should be considered such as portable capture hood, wet or dry vacuum machine equipped with a HEPA filter. Administrative control strategies can also be implemented such as adjust work schedules, education, training, good general hygiene, good housekeeping, and medical surveillance (NIOSH, 2011; NIOSH, 2012; NIOSH, 2013; OSHA 2013). More specifically, OSHA and NIOSH recommend using: RPE, protective

clothing, nitrile or chemically impervious gloves, and goggles. The RPE types recommended are N100, R100, and P100 for US (OSHA, 2013; OSHA, 2011; NIOSH, 2014) and P3 and filtering face piece (FFP3) for Europe (EN 143 and EN 149) (Goede et al., 2018; Rengasamy et al., 2009).

5. Conclusion

The airborne nano TiO_2 concentration was far greater than the labeled 2 wt% in the photocatalytic cement bag during simulation, increasing to 9.7 wt% during sweeping and 16.5 wt% during bag emptying. Work activities studied in the exposure chamber such as sweeping and bag emptying gave rise to nano TiO_2 air concentrations while concrete cutting did not. Thai and Swiss construction workers using regular cement had different exposure profiles. Thai workers were mostly exposed during sweeping and Swiss workers during drilling and polishing cement blocks. Both photocatalytic and regular cement had a GMD less than 3.5 µm thus will be able to penetrate into the lung. Emerging health risks associated with nano TiO_2 has yet to be assessed for construction workers using photocatalytic cement. We recommend workers using photocatalytic cement to use protection measures similar to recommendations made for nano TiO_2 exposures.

6. Conflict of interest

The authors declare no conflict of interest.

7. Acknowledgements

Funding was received from Center for Primary Care and Public Health (Unisanté), Department of Occupational and Environmental Health (formerly known as Institute for Work and Health, IST), Switzerland, the Royal Thai Government, and the Ministry of Science and Technology, Thailand. We greatly appreciate help from Dr. Nicolas Concha Lozano for the morphology, crystalline silica analysis, and elemental composition analysis. We would like to thank Ms. Nicole Charriere, Mr. Benoit Allaz, Mr. Nicolas Sambiagio, Mr. Timothée Ndarugendamwo, Mr. Elvar Oskarsson, Mr. Antoine Milon and Mr. Yannick Rodari for all practical laboratory and field support. We also thank the Laboratory of Construction Materials (LCM), at Swiss Federal Institute of Technology Lausanne (EPFL) for the x-ray diffraction characterization. We thank Italcementi group for sending us a free sample.

8. References

Aitken, R.J., K.S. Creely, and C.L. Tran. 2004. “Nanoparticles: An Occupational Hygiene Review.” Research Reports. http://www.hse.gov.uk/research/rrhtm/rr274.htm.

ANSES. 2019. “Titanium Dioxide in Nanoparticle Form: ANSES Defines a Toxicity Reference Value (TRV) for Chronic Inhalation Exposure.” French Agency for Food, Environmental and Occupational Health & Safety. https://www.anses.fr/en/content/titanium-dioxide-nanoparticle-form-anses-defines-toxicity-reference-value-trv-chronic.

Arenberg, Mary R., and Yuji Arai. 2020. “The Effects of Oxyanion Adsorption on Reactive Oxygen Species Generation by Titanium Dioxide.” Clays and Clay Minerals. https://doi.org/10.1007/s42860-019-00039-8.

Banerjee, Swagata, Dionysios D. Dionysiou, and Suresh C. Pillai. 2015. “Self-Cleaning Applications of TiO2 by Photo-Induced Hydrophilicity and Photocatalysis.” Applied Catalysis B: Environmental 176–177 (October): 396–428. https://doi.org/10.1016/j.apcatb.2015.03.058.

Batsungnoen, Kiattisak, Nancy B. Hopf, Guillaume Suárez, and Michael Riediker. 2019. “Characterization of Nanoparticles in Aerosolized Photocatalytic and Regular Cement.” Aerosol Science and Technology 53 (5): 540–48. https://doi.org/10.1080/02786826.2019.1578334.

Carp, O., C. L. Huisman, and A. Reller. 2004. “Photoinduced Reactivity of Titanium Dioxide.” Progress in Solid State Chemistry 32 (1–2): 33–177. https://doi.org/10.1016/j.progsolidstchem.2004.08.001.

Chen, Jun, and Chi-sun Poon. 2009. “Photocatalytic Construction and Building Materials: From Fundamentals to Applications.” Building and Environment 44 (9): 1899–1906. https://doi.org/10.1016/j.buildenv.2009.01.002.

Dalton, J. S, P. A Janes, N. G Jones, J. A Nicholson, K. R Hallam, and G. C Allen. 2002. "Photocatalytic Oxidation of NOx Gases Using TiO2: A Surface Spectroscopic Approach." Environmental Pollution 120 (2): 415–22. https://doi.org/10.1016/S0269-7491(02)00107-0.

Deurssen, Erik van, Anjoeka Pronk, Suzanne Spaan, Henk Goede, Erik Tielemans, Dick Heederik, and Tim Meijster. 2014. "Quartz and Respirable Dust in the Dutch Construction Industry: A Baseline Exposure Assessment as Part of a Multidimensional Intervention Approach." The Annals of Occupational Hygiene 58 (6): 724–38. https://doi.org/10.1093/annhyg/meu021.

Diesen, Veronica, and Mats Jonsson. 2014. "Formation of H2O2 in TiO2 Photocatalysis of Oxygenated and Deoxygenated Aqueous Systems: A Probe for Photocatalytically Produced Hydroxyl Radicals." The Journal of Physical Chemistry C 118 (19): 10083–87. https://doi.org/10.1021/jp500315u.

Ding, Yaobo, Thomas A. J. Kuhlbusch, Martie Van Tongeren, Araceli Sánchez Jiménez, Ilse Tuinman, Rui Chen, Iñigo Larraza Alvarez, et al. 2017. "Airborne Engineered Nanomaterials in the Workplace—a Review of Release and Worker Exposure during Nanomaterial Production and Handling Processes." Journal of Hazardous Materials, SI:Environmental Nanotechnol, 322 (January): 17–28. https://doi.org/10.1016/j.jhazmat.2016.04.075.

Edwin G. Foulke. 2008. Preventing Skin Problems from Working with Portland Cement. Occupational Safety and Health Administration, OSHA. https://www.osha.gov/Publications/OSHA-3351-portland-cement.pdf.

Eom, Sang-Yong, Eun-Bi Cho, Moo-Kyung Oh, Sun-Seog Kweon, Hae-Sung Nam, Yong-Dae Kim, and Heon Kim. 2017. “Increased Incidence of Respiratory Tract Cancers in People Living near Portland Cement Plants in Korea.” International Archives of Occupational and Environmental Health 90 (8): 859–64. https://doi.org/10.1007/s00420-017-1244-9.

Falck, G. C. M., H. K. Lindberg, S. Suhonen, M. Vippola, E. Vanhala, J. Catalán, K. Savolainen, and H. Norppa. 2009. “Genotoxic Effects of Nanosized and Fine TiO2.” Human & Experimental Toxicology 28 (6–7): 339–52. https://doi.org/10.1177/0960327109105163.

Friedlander, Sheldon K., and David Y. H. Pui. 2003. “National Science Foundation Workshop Report on Emerging Issues in Nanoparticle Aerosol Science and Technology (NAST).” Workshop Report. http://www.eng.uc.edu/~beaucag/Classes/MorphologyofComplexMaterials/NSFAerosolPar%20Report.pdf.

Fujishima, Akira, and Xintong Zhang. 2006. “Titanium Dioxide Photocatalysis: Present Situation and Future Approaches.” Comptes Rendus Chimie, Conversion photochimique et stockage de l’énergie solaire, 9 (5): 750–60. https://doi.org/10.1016/j.crci.2005.02.055.

Geiser, Marianne, and Wolfgang G. Kreyling. 2010. “Deposition and Biokinetics of Inhaled Nanoparticles.” Particle and Fibre Toxicology 7: 2. https://doi.org/10.1186/1743-8977-7-2.

Ghosh, Manosij, Maumita Bandyopadhyay, and Anita Mukherjee. 2010. “Genotoxicity of

Titanium Dioxide (TiO2) Nanoparticles at Two Trophic Levels: Plant and Human Lymphocytes." Chemosphere 81 (10): 1253–62. https://doi.org/10.1016/j.chemosphere.2010.09.022.

Goede, Henk, Yvette Christopher-de Vries, Eelco Kuijpers, and Wouter Fransman. 2018. "A Review of Workplace Risk Management Measures for Nanomaterials to Mitigate Inhalation and Dermal Exposure." Annals of Work Exposures and Health. https://doi.org/10.1093/annweh/wxy032.

Guillemin, Michel. 1975. "Mise Au Point et Utilisation d'une Cabine d'expérimentation." Archives Des Maladies Professionnelles de Medecine Du Travail et de Securite Sociale (Paris) (Arch. Mal. Prof.) 36: 421–28.

IARC. 1997. IARC Monographs on the Evaluation of Carcinogenic Risk to Human Silica, Some Silicates, Coal Dust and Para-Aramid Fibrils. Vol. 68. World health organization, International Agency for Research on Cancer. http://monographs.iarc.fr/ENG/Monographs/vol68/.

IARC. 2012. Silica Dust Crystalline in the Form of Quartz or Cristobalite. World health organization, International Agency for Research on Cancer. https://monographs.iarc.fr/ENG/Monographs/vol100C/mono100C-14.pdf.

IARC. 2017. IARC Monographs on the Evaluation of Carcinogenic Risk to Human; List of Classification. Vol. 1–120. World health organization, International Agency for Research on Cancer. http://monographs.iarc.fr/ENG/Classification/latest_classif.php.

ICRP. 1994. "Human Respiratory Tract Model for Radiological Protection. A Report of a Task Group of the International Commission on Radiological Protection." Annals of the ICRP 24 (1–3): 1–482.

ILO. 2014. "Safety and Health in the Construction Sector- Overcoming the Challenges."

Event. October 2, 2014. http://www.ilo.org/empent/Eventsandmeetings/WCMS_310993/lang--en/index.htm.

Jimenez-Relinque, E., J. R. Rodriguez-Garcia, A. Castillo, and M. Castellote. 2015. "Characteristics and Efficiency of Photocatalytic Cementitious Materials: Type of Binder, Roughness and Microstructure." Cement and Concrete Research 71 (May): 124–31. https://doi.org/10.1016/j.cemconres.2015.02.003.

Kaewamatawong, Theerayuth, Natsuko Kawamura, Mina Okajima, Masumi Sawada, Takehito Morita, and Akinori Shimada. 2005. "Acute Pulmonary Toxicity Caused by Exposure to Colloidal Silica: Particle Size Dependent Pathological Changes in Mice." Toxicologic Pathology 33 (7): 745–51. https://doi.org/10.1080/01926230500416302.

Kokkonen, Anna, Markku Linnainmaa, Arto Säämänen, Tomi Kanerva, Jouni Sorvari, Mikko Kolehmainen, Vuokko Lappalainen, and Pertti Pasanen. 2019. "Control of Dust Dispersion From an Enclosed Renovation Site Into Adjacent Areas by Using Local Exhaust Ventilation." Annals of Work Exposures and Health. https://doi.org/10.1093/annweh/wxz016.

Kreyling, Wolfgang G, Stephanie Hirn, and Carsten Schleh. 2010. "Nanoparticles in the Lung." Nature Biotechnology 28 (12): 1275–76. https://doi.org/10.1038/nbt.1735.

Kwon, Soonjin, Young-Su Yang, Hyo-Seon Yang, Jinsoo Lee, Min-Sung Kang, Byoung-seok Lee, Kyuhong Lee, and Chang-Woo Song. 2012. "Nasal and Pulmonary Toxicity of Titanium Dioxide Nanoparticles in Rats." Toxicological Research 28 (4): 217–24. https://doi.org/10.5487/TR.2012.28.4.217.

Lan, Yucheng, Yalin Lu, and Zhifeng Ren. 2013. "Mini Review on Photocatalysis of

Titanium Dioxide Nanoparticles and Their Solar Applications." Nano Energy 2 (5): 1031–45. https://doi.org/10.1016/j.nanoen.2013.04.002.

Lee, Jaesang, Shaily Mahendra, and Pedro J. J. Alvarez. 2010. "Nanomaterials in the Construction Industry: A Review of Their Applications and Environmental Health and Safety Considerations." ACS Nano 4 (7): 3580–90. https://doi.org/10.1021/nn100866w.

Lim, Tak Hyoung, Sang Mun Jeong, Sang Done Kim, and Janos Gyenis. 2000. "Photocatalytic Decomposition of NO by TiO2 Particles." Journal of Photochemistry and Photobiology A: Chemistry 134 (3): 209–17. https://doi.org/10.1016/S1010-6030(00)00265-3.

Long, Thomas C., Navid Saleh, Robert D. Tilton, Gregory V. Lowry, and Bellina Veronesi. 2006. "Titanium Dioxide (P25) Produces Reactive Oxygen Species in Immortalized Brain Microglia (BV2): Implications for Nanoparticle Neurotoxicity." Environmental Science & Technology 40 (14): 4346–52.

Ma, Baoguo, Hainan Li, Junpeng Mei, Xiangguo Li, and Fangjie Chen. 2015. "Effects of Nano-TiO2 on the Toughness and Durability of Cement-Based Material." Advances in Materials Science and Engineering. https://doi.org/10.1155/2015/583106.

Ma, Hongbo, Amanda Brennan, and Stephen A. Diamond. 2012. "Photocatalytic Reactive Oxygen Species Production and Phototoxicity of Titanium Dioxide Nanoparticles Are Dependent on the Solar Ultraviolet Radiation Spectrum." Environmental Toxicology and Chemistry 31 (9): 2099–2107. https://doi.org/10.1002/etc.1916.

Maciejewska, A., and G. Bielichowska-Cybula. 1991. "[Biological effect of cement dust]."

Medycyna Pracy 42 (4): 281–89.

McLaughlin, J. K., W. H. Chow, and L. S. Levy. 1997. “Amorphous Silica: A Review of Health Effects from Inhalation Exposure with Particular Reference to Cancer.” Journal of Toxicology and Environmental Health 50 (6): 553–66. https://doi.org/10.1080/15287399709532054.

McLean, David, Bill Glass, Andrea ’t Mannetje, and Jeroen Douwes. 2017. “Exposure to Respirable Crystalline Silica in the Construction Industry-Do We Have a Problem?” The New Zealand Medical Journal 130 (1466): 78–82.

Meo, Sultan A. 2004. “Health Hazards of Cement Dust.” Saudi Medical Journal 25 (9): 1153–

59.

Merget, R., T. Bauer, H. U. Küpper, S. Philippou, H. D. Bauer, R. Breitstadt, and T. Bruening. 2002. “Health Hazards Due to the Inhalation of Amorphous Silica.” Archives of Toxicology 75 (11–12): 625–34.

Moghadam, Somayeh Rahimi, Siavosh Abedi, Mahdi Afshari, Ehsan Abedini, and Mahmood Moosazadeh. 2017. “Decline in Lung Function among Cement Production Workers: A Meta-Analysis.” Reviews on Environmental Health 32 (4): 333–341. https://doi.org/10.1515/reveh-2017-0017.

Napierska, Dorota, Leen CJ Thomassen, Dominique Lison, Johan A Martens, and Peter H Hoet. 2010. “The Nanosilica Hazard: Another Variable Entity.” Particle and Fibre Toxicology 7 (December): 39. https://doi.org/10.1186/1743-8977-7-39.

NIOSH. 1998. “NIOSH Manual of Analytical Methods 0600: Particulate Not Otherwise Regulated, Respirable.” The National Institute for Occupational Safety and Health (NIOSH). https://www.cdc.gov/niosh/docs/2003-154/method-cas0.html.

NIOSH. 2003. “NIOSH Manual of Analytical Methods 7602: Silica, Crystalline by IR (KBr

Pellet).” The National Institute for Occupational Safety and Health (NIOSH). https://www.cdc.gov/niosh/docs/2003-154/method-cas1.html.

NIOSH. 2009. Approaches to Safe Nanotechnology Managing the Health and Safety Concerns Associated with Engineered Nanomaterials. U.S. Department of Health and Human Services, Centers for Disease Control and Prevention, National Institute for Occupational Safety and Health. http://www.cdc.gov/niosh/docs/2009-125/pdfs/2009-125.pdf.

NIOSH. 2011. Occupational Exposure to Titanium Dioxide. U.S. Department of Health and Human Services, Centers for Disease Control and Prevention, National Institute for Occupational Safety and Health.

NIOSH. 2012. General Safe Practices for Working with Engineered Nanomaterials in Research Laboratories. U.S. Department of Health and Human Services, Centers for Disease Control and Prevention, National Institute for Occupational Safety and Health. http://www.cdc.gov/niosh/docs/2012-147/pdfs/2012-147.pdf.

NIOSH. 2013. Current Strategies for Engineering Controls in Nanomaterial Production and Downstream Handling Processes. U.S. Department of Health and Human Services, Centers for Disease Control and Prevention, National Institute for Occupational Safety and Health. http://www.cdc.gov/niosh/docs/2014-102/pdfs/2014-102.pdf.

NIOSH. 2014. “NIOSH Guide to the Selection and Use of Particulate Respirators, Certified

Under 42 CFR 84." U.S. Department of Health and Human Services, Centers for Disease Control and Prevention, National Institute for Occupational Safety and Health. http://www.cdc.gov/niosh/docs/96-101/.

NIOSH. 2018. "NIOSH Pocket Guide to Chemical Hazards: Silica, Amorphous." The National Institute for Occupational Safety and Health (NIOSH). https://www.cdc.gov/index.htm.

NJDHSS. 2003. "Hazardous Substances Fact Sheet: Calcium Oxide." New Jersey Department of Health and Senior Services. https://nj.gov/health/eoh/rtkweb/documents/fs/0325.pdf.

Noël, A., K. Maghni, Y. Cloutier, C. Dion, K. J. Wilkinson, S. Hallé, R. Tardif, and G. Truchon. 2012. "Effects of Inhaled Nano-TiO2 Aerosols Showing Two Distinct Agglomeration States on Rat Lungs." Toxicology Letters 214 (2): 109–19. https://doi.org/10.1016/j.toxlet.2012.08.019.

Nordby, K.-C., A. K. M. Fell, H. Notø, W. Eduard, M. Skogstad, Y. Thomassen, A. Bergamaschi, J. Kongerud, and H. Kjuus. 2011. "Exposure to Thoracic Dust, Airway Symptoms and Lung Function in Cement Production Workers." The European Respiratory Journal 38 (6): 1278–86. https://doi.org/10.1183/09031936.00007711.

Notø, Hilde, Karl-Christian Nordby, Helge Kjuus, Øivind Skare, Yngvar Thomassen, and Wijnand Eduard. 2015. "Exposure to Thoracic Aerosol in a Prospective Lung Function Study of Cement Production Workers." The Annals of Occupational Hygiene 59 (1): 4–24. https://doi.org/10.1093/annhyg/meu080.

Oberdörster, Günter, Eva Oberdörster, and Jan Oberdörster. 2005. "Nanotoxicology: An

Emerging Discipline Evolving from Studies of Ultrafine Particles." Environmental Health Perspectives 113 (7): 823–39.

OSHA. 2011. "Respiratory Protection. - 1910.134." U.S. Department of Labor, Occupational Safety and Health Administration. https://www.osha.gov/pls/oshaweb/owadisp.show_document?p_table=STANDARDS&p_id=12716.

OSHA. 2013. "Working Safely with Nanomaterials." U.S. Department of Labour, Occupational Safety and Health Administration. https://www.osha.gov/Publications/OSHA_FS-3634.pdf.

OSHA. 2018. "Occupational Exposure Limits (OELs)." Occupational Safety and Health Administration. https://www.osha.gov/dsg/annotated-pels/tablez-1.html.

Ostiguy, C., G. Lapointe, L. Ménard, Y. Cloutier, M. Trottier, M. Boutin, M. Antoun, and C. Normand. 2006. "Nanoparticles - Actual Knowledge about Occupational Health and Safety Risks and Prevention Measures." Research Reports. https://www.irsst.qc.ca/en/publications-tools/publication/i/100189/n/nanoparticles-current-knowledge-about-occupational-health-and-safety-risks-and-prevention-measures-r-470.

Paz, Y., Z. Luo, L. Rabenberg, and A. Heller. 1995. "Photooxidative Self-Cleaning Transparent Titanium Dioxide Films on Glass." Journal of Materials Research 10 (11): 2842–48. https://doi.org/10.1557/JMR.1995.2842.

Penrose, Beris. 2014. "Occupational Exposure to Cement Dust: Changing Opinions of a Respiratory Hazard." Health and History 16 (1): 25–44.

Qi, Chaolong, Alan Echt, and Michael G. Gressel. 2017. "The Generation Rate of Respirable Dust from Cutting Fiber Cement Siding Using Different Tools." Annals of Work Exposures and Health 61 (2): 218–25. https://doi.org/10.1093/annweh/wxw010.

Rengasamy, Samy, Benjamin C. Eimer, and Ronald E. Shaffer. 2009. “Comparison of Nanoparticle Filtration Performance of NIOSH-Approved and CE-Marked Particulate Filtering Facepiece Respirators.” The Annals of Occupational Hygiene 53 (2): 117–28. https://doi.org/10.1093/annhyg/men086.

Ringen, Knut, John Dement, Laura Welch, Xiuwen Sue Dong, Eula Bingham, and Patricia S. Quinn. 2014. “Risks of a Lifetime in Construction. Part II: Chronic Occupational Diseases.” American Journal of Industrial Medicine 57 (11): 1235–45. https://doi.org/10.1002/ajim.22366.

Sayes, Christie M., Rajeev Wahi, Preetha A. Kurian, Yunping Liu, Jennifer L. West, Kevin D. Ausman, David B. Warheit, and Vicki L. Colvin. 2006. “Correlating Nanoscale Titania Structure with Toxicity: A Cytotoxicity and Inflammatory Response Study with Human Dermal Fibroblasts and Human Lung Epithelial Cells.” Toxicological Sciences 92 (1): 174–85. https://doi.org/10.1093/toxsci/kfj197.

Sha, Baoyong, Wei Gao, Xingye Cui, Lin Wang, and Feng Xu. 2015. “The Potential Health Challenges of TiO2 Nanomaterials.” Journal of Applied Toxicology: JAT, July. https://doi.org/10.1002/jat.3193.

Shi, Hongbo, Ruth Magaye, Vincent Castranova, and Jinshun Zhao. 2013. “Titanium Dioxide Nanoparticles: A Review of Current Toxicological Data.” Particle and Fibre Toxicology 10 (April): 15. https://doi.org/10.1186/1743-8977-10-15.

Shinohara, Naohide, Yutaka Oshima, Toshio Kobayashi, Nobuya Imatanaka, Makoto Nakai, Takayuki Ichinose, Takeshi Sasaki, Kenji Kawaguchi, Guihua Zhang, and Masashi Gamo. 2015. “Pulmonary Clearance Kinetics and Extrapulmonary Translocation of Seven Titanium Dioxide Nano- and Submicron Materials Following Intratracheal

Administration in Rats." Nanotoxicology 9 (8): 1050–58. https://doi.org/10.3109/17435390.2015.1015644.

Soutar, C. A., A. Robertson, B. G. Miller, A. Searl, and J. Bignon. 2000. "Epidemiological Evidence on the Carcinogenicity of Silica: Factors in Scientific Judgement." Annals of Occupational Hygiene 44 (1): 3–14. https://doi.org/10.1093/annhyg/44.1.3.

Tedja, Roslyn, Christopher Marquis, May Lim, and Rose Amal. 2011. "Biological Impacts of TiO2 on Human Lung Cell Lines A549 and H1299: Particle Size Distribution Effects." Journal of Nanoparticle Research 13 (9): 3801–13. https://doi.org/10.1007/s11051-011-0302-6.

TOXNET. 2014. "Calcium Oxide." Toxicology data network, US National Library of Medicine. https://toxnet.nlm.nih.gov/cgi-bin/sis/search2/r?dbs+hsdb:@term+@DOCNO+1615.

Wang, Jiangxue, Chunying Chen, Ying Liu, Fang Jiao, Wei Li, Fang Lao, Yufeng Li, et al. 2008. "Potential Neurological Lesion after Nasal Instillation of TiO2 Nanoparticles in the Anatase and Rutile Crystal Phases." Toxicology Letters 183 (1–3): 72–80. https://doi.org/10.1016/j.toxlet.2008.10.001.

Wang, Jiangxue, and Yubo Fan. 2014. "Lung Injury Induced by TiO2 Nanoparticles Depends on Their Structural Features: Size, Shape, Crystal Phases, and Surface Coating." International Journal of Molecular Sciences 15 (12): 22258–78. https://doi.org/10.3390/ijms151222258.

WHO. 2010. IARC Monographs on the Evaluation of Carcinogenic Risks to Humans: Carbon Black, Titanium Dioxide, and Talc. Vol. 93. World health organization, International Agency for Research on Cancer. http://monographs.iarc.fr/ENG/Monographs/vol93/mono93.pdf.

Xue, Chengbin, Wen Luo, and Xiang liang Yang. 2015. “A Mechanism for Nano-Titanium Dioxide-Induced Cytotoxicity in HaCaT Cells under UVA Irradiation.” Bioscience, Biotechnology, and Biochemistry 79 (8): 1384–90. https://doi.org/10.1080/09168451.2015.1023248.

Xue, Jian, Yang Li, Xiaoliang Wang, Thomas D. Durbin, Kent C. Johnson, Georgios Karavalakis, Akua Asa-Awuku, et al. 2015. “Comparison of Vehicle Exhaust Particle Size Distributions Measured by SMPS and EEPS During Steady-State Conditions.” Aerosol Science and Technology 49 (10): 984–96. https://doi.org/10.1080/02786826.2015.1088146.

Yang, C. Y., C. C. Huang, H. F. Chiu, J. F. Chiu, S. J. Lan, and Y. C. Ko. 1996. “Effects of Occupational Dust Exposure on the Respiratory Health of Portland Cement Workers.” Journal of Toxicology and Environmental Health 49 (6): 581–88.

Yang, Lu, Amer Hakki, Fazhou Wang, and Donald E. Macphee. 2018. “Photocatalyst Efficiencies in Concrete Technology: The Effect of Photocatalyst Placement.” Applied Catalysis B: Environmental 222 (March): 200–208. https://doi.org/10.1016/j.apcatb.2017.10.013.

Zeleke, Zeyede K., Bente E. Moen, and Magne Bråtveit. 2011. “Excessive Exposure to Dust among Cleaners in the Ethiopian Cement Industry.” Journal of Occupational and Environmental Hygiene 8 (9): 544–50. https://doi.org/10.1080/15459624.2011.601711.

Zhi Ge, and Zhili Gao. 2008. “Applications of Nanotechnology and Nanomaterials in Construction.” First International Conference on Construction In Developing Countries (ICCIDC–I). http://www.neduet.edu.pk/Civil/ICCIDC-I/Conference%20Proceedings/Papers/025.pdf.

Zhu, W., P. J. M. Bartos, and A. Porro. 2004. “Application of Nanotechnology in Construction.” Materials and Structures 37 (9): 649–58. https://doi.org/10.1007/BF02483294.

Zouzelka, Radek, and Jiri Rathousky. 2017. “Photocatalytic Abatement of NOx Pollutants in the Air Using Commercial Functional Coating with Porous Morphology.” Applied Catalysis B: Environmental 217 (November): 466–76. https://doi.org/10.1016/j.apcatb.2017.06.009.